Electronic Supplementary Material (ESI) for ChemComm.

Supporting Information

Enhancing the selectivity of optical sensors using synthetic transmembrane ion transporters

Sarah R. Marshall, Anmol Singh, Jacqueline N. Wagner, Nathalie Busschaert*

Department of Chemistry, Tulane University, New Orleans, Louisiana 70118, United States, nbusschaert@tulane.edu

Table of Contents

S1. General

^{1}H NMR (500 MHz) spectra were collected on a Bruker 500 MHz NMR and ^{13}C NMR (75 MHz) spectra were determined on a Bruker Avance 300 spectrometer. ^{13}C NMR spectra were collected proton decoupled. Chemical shifts (δ) are reported in parts per million (ppm) and calibrated to the residual solvent peak in DMSO-d_6 (δ = 2.50 (^{1}H) and 39.5 ppm (^{13}C)). The following abbreviations are used for spin multiplicity: s = singlet, d = doublet. High resolution electron spray ionization (ESI) mass spectra were recorded on a Bruker micrOTOF. Infrared (IR) spectra were recorded on a Nexus 670 Avatar FTIR spectrometer; only a selected number of the most pronounced peaks are reported. Elemental analysis was conducted by *Midwest Laboratories Inc*. HPLC traces were collected on a Thermo Fisher Scientific Vanquish Flex UHPLC with variable wavelength detector, using a Hypersil GOLD C18 column (150 mm length, 3.0 mm diameter, 3 µm particle size). Fluorescence spectra and kinetic studies were performed on an Agilent Cary Eclipse fluorescence spectrophotometer equipped with stirring function and Peltier temperature controller. 3 mL macrocuvettes (quartz or glass) were used and all solutions were stirred using a cuvette stir bar (Sigma-Aldrich #Z363545). Solvents, reagents and inorganic salt were used as provided by the supplier. Buffers were prepared using fresh UltraPure water.

S2. Original anion selectivity of lucigenin

To a solution of 0.25 µM lucigenin in nitrate buffer (222 mM $NaNO_3$, 5 mM HEPES, pH 7.4) was added 16.4 mM of a variety of sodium salts. The fluorescence spectrum (excitation 430 nm) was measured before and after addition of the salt. The spectra were normalized by dividing the fluorescence intensity at any wavelength by the fluorescence intensity at 505 nm before the addition of salt (**Figure S1**). The experiment was repeated at least 3 times. The percent of fluorescence quenching was calculated using the fluorescence intensity at 505 nm (F_{505nm}). The obtained percent of fluorescence quenching values are given in **Table S1**, and a bar graph is given in **Figure S2**.

$$\%\ quenching = \left(1 - \frac{F_{505nm}\ after\ addition\ salt}{F_{505nm}\ before\ addition\ salt}\right) \cdot 100\%$$

Table S1. % lucigenin fluorescence quenching by a variety of sodium salts. Errors are standard deviation

Anion	% quenching (505 nm)
fluoride	2.74 ± 0.93
chloride	60.21 ± .42
bromide	73.86 ± 0.19
iodide	78.61 ± 0.29
nitrate	3.84 ± 0.25
sulfate	6.34 ± 0.65
phosphate	-2.1 ± 1.4
perchlorate	-0.10 ± 0.32
bicarbonate	12.41 ± 0.22
acetate	16.9 ± 2.3
gluconate	13.43 ± 0.85
ascorbate	49.73 ± 0.51

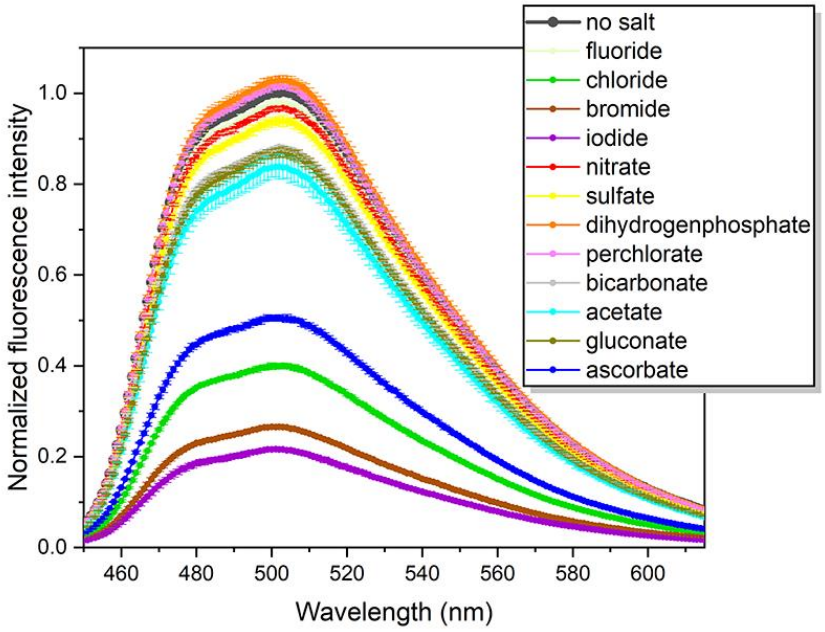

Figure S1. Normalized fluorescence spectra of lucigenin in the presence of a variety of sodium salts (0.25 µM lucigenin, 222 mM $NaNO_3$, 5 mM HEPES, pH 7.4, 16.4 mM sodium salt). The excitation wavelength was 430 nm. Results are the average of 3 repeats and error bars represent standard deviations.

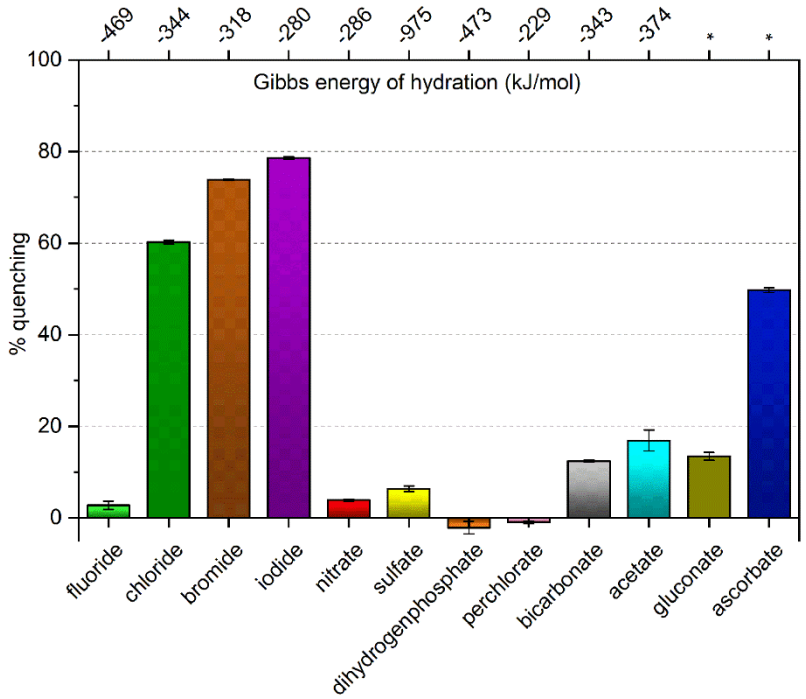

Figure S2. The percent of fluorescence quenching of a solution of 0.25 µM lucigenin in nitrate buffer (222 mM $NaNO_3$, 5 mM HEPES, pH 7.4 in the presence of 16.4 mM sodium salts. The excitation wavelength was set to 430 nm and the fluorescence intensity was measured at 505 nm. Values are the average of 3 repeats and the error bars represent standard deviations. The top x-axis shows the Gibbs energy of hydration for the respective anions; values were taken from *Y. Marcus, Ions in Solution and their Solvation*[1] (* hydration energies of ascorbate and gluconate are not known, but are assumed to be strongly negative due to multiple hydroxyl and carboxylate functionalities).

S3. Synthesis and characterization of compound 5

Compounds **1-4** were synthesized as previously reported.[2-4] Compound **5** was synthesized as follows: 4-Methylsulfonylaniline (0.856 µg, 5 mmol) was dissolved in a minimal amount of DMF. To this colorless solution was added 1,1'-carbonyldiimidazole (0.5 eq, 0.405 g, 2.5 mmol) and diisopropylethylamine (100 µL). The reaction was stirred under inert gas overnight. The clear, colorless solution was diluted with a minimal amount of water, affording a white solid. The precipitate was collected over a fine fritted funnel, and subsequently purified using column chromatography (silica gel) using a gradient of 1:1 ethyl acetate:hexane to 100% ethyl acetate to 10% methanol in ethyl acetate. Due to the low solubility of the compound, a large amount of solvent was needed recover the compound from the column. After drying overnight under high vacuum, compound **5** was obtained as a white solid (168 mg, 0.46 mmol). Yield: 18%. ^{1}H NMR (500 MHz, DMSO-d_6) δ 3.16 (s, 6 H), 7.71 (d, J = 8 Hz, 4 H), 7.84 (d, J = 8 Hz, 4 H), 9.38 (s, 2 H) ppm. ^{13}C NMR (75 MHz, DMSO-d_6) δ 43.9, 118.0, 128.3, 133.6, 144.0, 151.9 ppm. FTIR (solid): ν = 3338 (weak, br), 1712, 1589, 1531, 1317, 1296, 1282, 1201, 1137 cm^{-1}. HRMS (ESI-) for $C_{15}H_{15}N_2O_5S_2$ [M-H]$^-$: m/z = 367.0433 (calc), 367.0299 (found). Elemental analysis for $C_{15}H_{16}N_2O_5S_2$: C 48.90%, H 4.38%, N 7.60%, O 21.71%, S 17.40% (calc), C 48.87%, H 4.33%, N 7.71%, O 21.67%, S 17.42% (found).

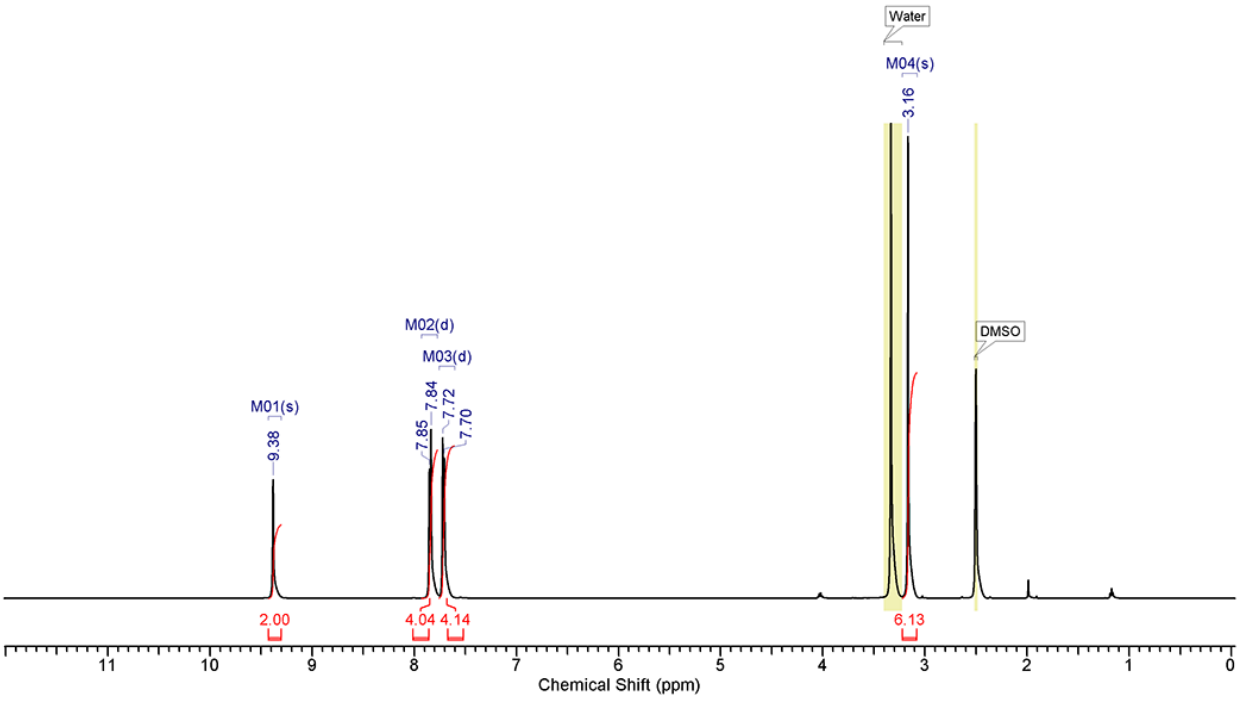

Figure S3. ^{1}H NMR (500 MHz) spectrum of compound **5** in DMSO-d_6 at 298 K.

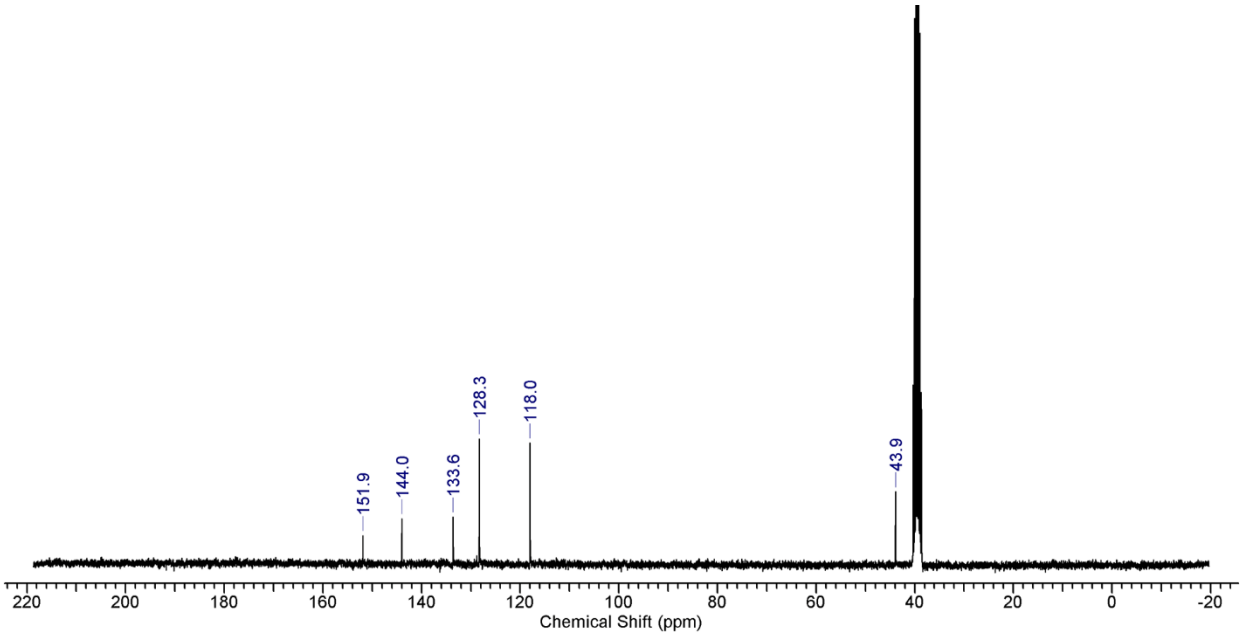

Figure S4. ^{13}C NMR (75 MHz) spectrum of compound **5** in DMSO-d_6 at 298 K.

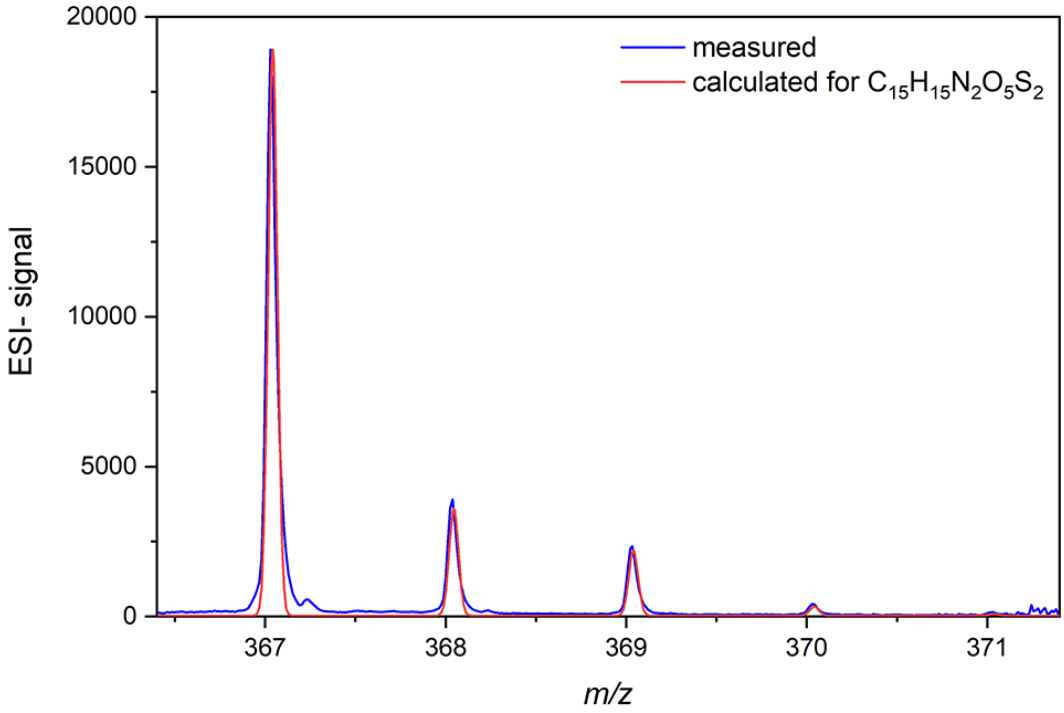

Figure S5. ESI-spectrum of compound **5** overlaid with the theoretical spectrum for $C_{15}H_{15}O_5N_2S_2$

S4. HPLC traces and lipophilicity of compounds 1-5

HPLC traces were collected on a Thermo Fisher Scientific Vanquish Flex UHPLC with variable wavelength detector, using a Hypersil GOLD C18 column (150 mm length, 3.0 mm diameter, 3 µm particle size). 'Solvent A' was 20 mM phosphate buffer (pH 7.4) and 'solvent B' was acetonitrile. Gradient was from 5% B to 95% B in 9 min, followed by 2 minutes at 95% B and 4 minutes at 5% B. Detection wavelength was set at 250 nm. Compounds **1-5** were dissolved in DMSO and subsequently diluted in acetonitrile/water until dissolved, before injecting into the UHPLC. The samples were run 3 times. The results are shown in **Figures S6-S10**.

Octanol-water partition coefficients (log*P* values) were calculated using ChemDraw 16.0.1.4 (logP and ClogP), Pubchem ClogP (https://pubchem.ncbi.nlm.nih.gov/, accessed May 2020) and Molinspirations ClogP (https://www.molinspiration.com/cgi-bin/properties, accessed June 2020). The values are given in **Table S2**. Due to the small number of compounds, all calculated log*P* values showed a linear correlation with the HPLC retention time with an R-value ~0.9. However, the log*P* values calculated by Chemdraw were the only ones that predicted the correct relative lipophilicity of the compounds based on HPLC: SO_2Me (**5**) << OMe (**1**) < H (**2**)< CN (**4**) << CF_3 (**3**), where SO_2Me (compound **5**) is the most polar compound.

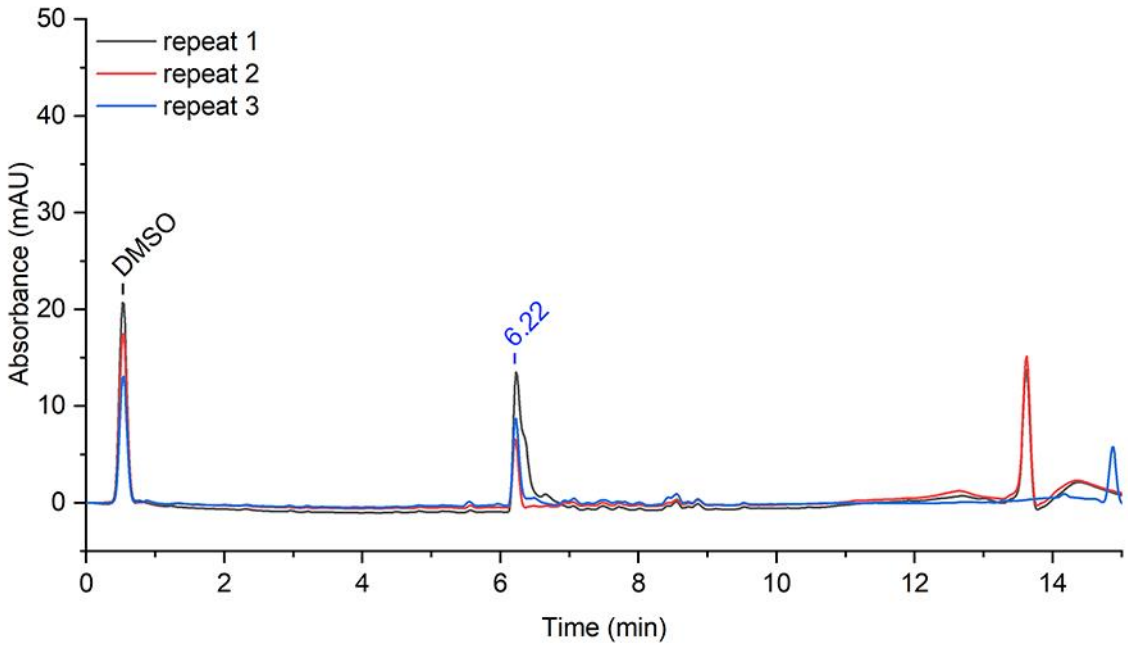

Figure S6. Reverse-phase HPLC of compound **1.**

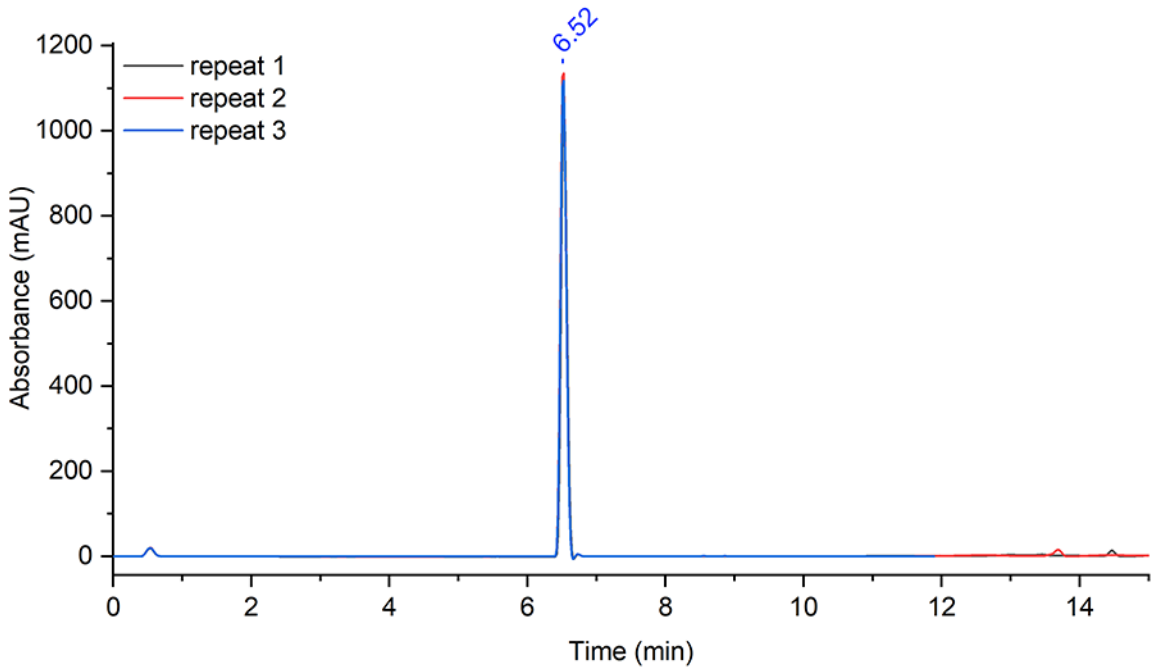

Figure S7. Reverse-phase HPLC of compound **2.**

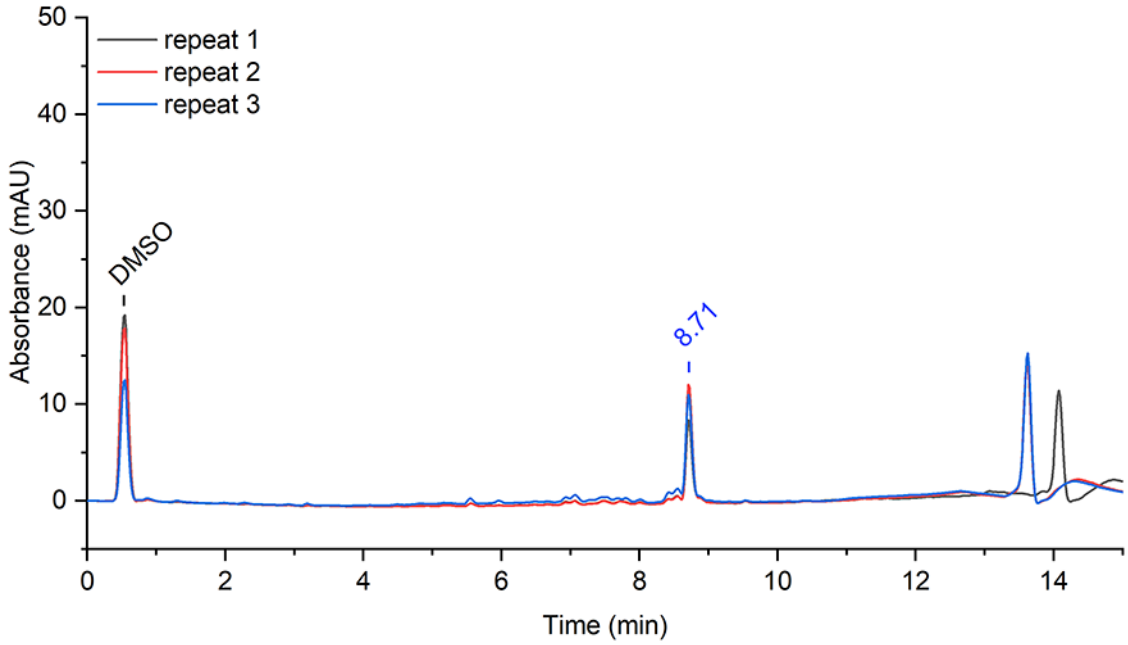

Figure S8. Reverse-phase HPLC of compound **3.**

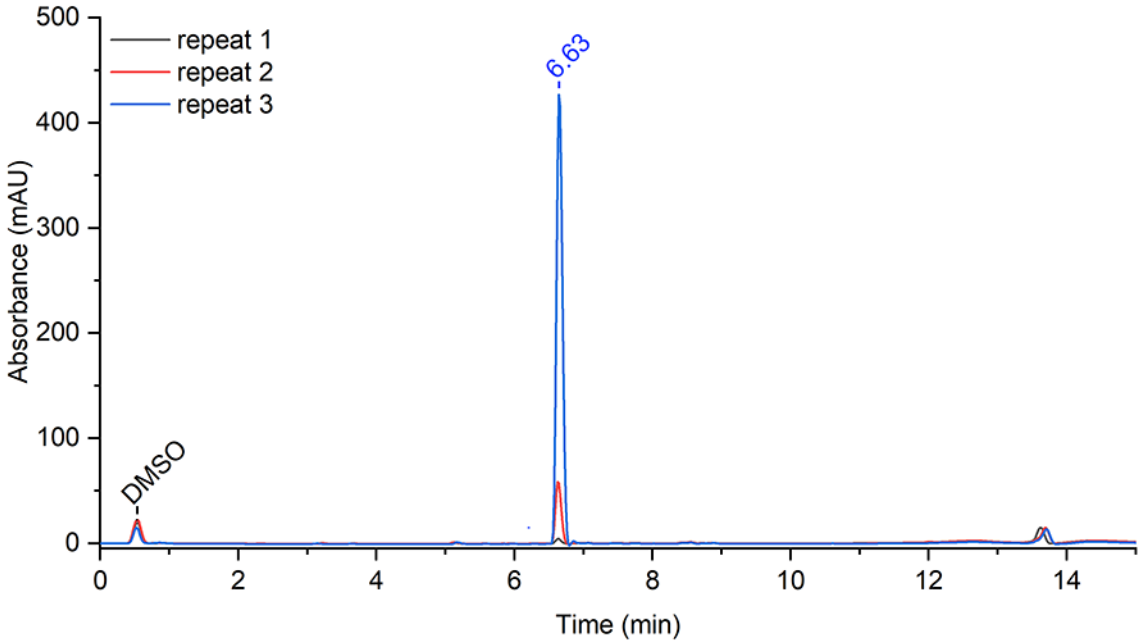

Figure S9. Reverse-phase HPLC of compound **4.**

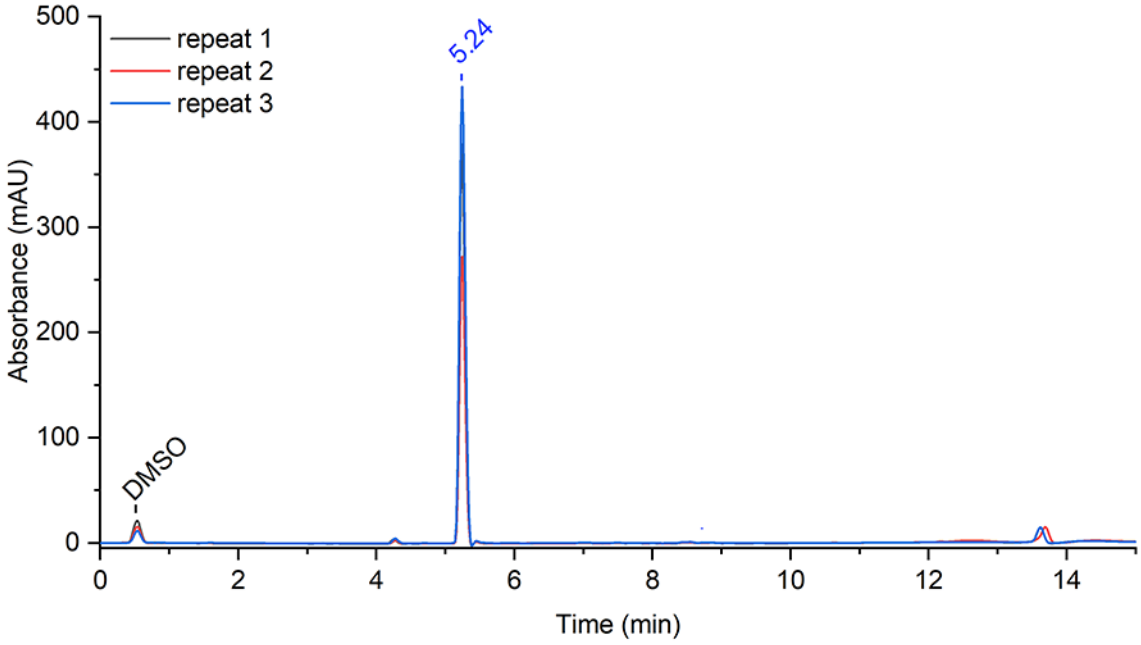

Figure S10. Reverse-phase HPLC of compound **5.**

Table S2. Overview of the Hammett constant for substituents in the *para*-position, experimental retention times on reverse-phase HPLC, and various calculated log*P* values for compounds **1-5**.

Compound	Hammett	RT (min)	Clog*P* Chemdraw	log*P* Chemdraw	Clog*P* Pubchem	Molinspiration
1 (OMe)	-0.27	6.22	3.09586	2.26	2.9	3.26
2 (H)	0	6.52	3.01	2.51	3	3.14
3 (CF_3)	0.54	8.71	5.49042	4.36	4.8	4.93
4 (CN)	0.66	6.63	2.8237	2.58	2.4	2.65
5 (SO_2Me)	0.72	5.24	0.7486	-0.08	-	0.88

S5. Experimental procedure for liposome preparation and anion transport assays

The procedures for the various membrane transport assays mentioned in the article are described. EggPC (egg (chicken) phosphatidylcholine), was ordered from *Avanti Polar Lipids, Inc.* (catalog# 840051), and stored as a solution in chloroform (1 g in 35 mL chloroform) at -20°C. Buffer was prepared with fresh UltraPure water and the composition was calculated for a 5 mM HEPES buffer, pH 7.4, 25 ^{o}C with an ionic strength of 225 mM, using an online tool (https://www.biomol.net/en/tools/buffercalculator.htm). All other salts and reagents were used a provided by the manufacturer. Stock solutions of transporters **1-5** were made in DMF at six different concentrations. Stock solutions of the analytes (various sodium salts) were prepared as 1 M stock solutions in water. The kinetic assays were performed on an Agilent Cary Eclipse fluorometer, using an excitation wavelength of 430 nm and emission wavelength of 505 nm.

S5.1. Preparation of large unilamellar vesicles

An aliquot of the lipid stock solution in chloroform was transferred to a small round bottom flask and dried via rotary evaporation. The lipid film was dried further on high vacuum for at least 5 hours prior to use. The lipid film was hydrated with the internal solution (1 mM lucigenin, 222 mM $NaNO_3$, 5 mM HEPES buffer at pH 7.4) and vortexed for about 5 minutes. The resulting suspension was subjected to seven freeze-thaw cycles, alternating between submersion in liquid nitrogen followed by thawing in mildly warm water. The lipid suspension was allowed to rest at room temperature for 30 minutes before extruding 25 times through a 100 nm polycarbonate membrane (*Nucleopore*) using the Avanti mini extruder set (*Avanti Polar Lipids, Inc.*). The resulting uniform large unilamellar vesicles (LUVs) were separated from the unencapsulated lucigenin by size exclusion chromatography using a Sephadex column (G-50, medium). The obtained concentrated stock liposome solution was diluted in external buffer (222 mM $NaNO_3$, 5 mM HEPES buffer at pH 7.4) to afford a final lipid concentration of 0.5 mM.

S5.2. Anion transport kinetic assays

The lucigenin-loaded liposomes (0.5 mM lipid) were transferred to a 3 mL fluorescence cuvette and a small cuvette stir bar was added. The cuvette was placed in the fluorometer and stirring was started at maximum speed (stirring continued throughout the experiment). 50 Seconds before the start of the kinetic run, 75 µL NaX stock solution was added to achieve a final concentration of 25 mM sodium

salt. At time *t* = 0 s, the kinetic run was started and the fluorescence intensity at 505 nm (excitation 430 nm) was measured for 400 s. At time *t* = 10 s, 7.5 µL transporter in DMF was added to initiate the influx of X^- anions and the efflux of NO_3^- anions. At time t = 330 s, detergent (75 µL of 10% Triton X-100) was added to fully lyse the membrane and estimate the quality of the liposomes. Transporter concentrations are given as mol% with respect to EggPC lipid concentration.

S5.3. Calculation of initial rate of transport

The crude kinetic run was first normalized as F/F_0 (where F is the fluorescence intensity at any time, and F_0 is the fluorescence intensity at time *t* = 0 s). The time scale was also corrected to ensure that anion transport starts at time 0 (because the transporter was added after 10 s, this indicates shifting the time scale with 10 seconds). The final F/F_0 versus time trace was subjected to an asymptotic fit using OriginPro 2019 (where t = time, and a, b and c are parameters):

$$\frac{F}{F_0} = a - bc^t$$

The absolute initial rate of transport is then given by the first derivative at time *t* = 0 s, corresponding to $|b \cdot ln(c)|$. If anion transport was too slow are too fast, asymptotic fits were not possible and the data was fitted using a linear fit. In this case, the absolute initial rate of transport is given by the absolute value of the slope of the linear fit.

S6. Identification of TLF system with the best iodide selectivity

To identify the TLF system with the best iodide selectivity, the experiment described in Section S5 was conducted for the sodium salts NaF, NaCl, NaBr and NaI (final concentrations 25 mM) with various concentrations of transporters **1-5**. **Figure S11-Figure S15** show the corrected F/F_0 traces obtained for these experiments. All experiments are the average of a minimum of 3 independent repeats (using different batches of liposomes), and error bars indicate standard deviations. The calculated initial rate of transport ($|k_{ini}|$ values) are given in **Table S3-Table S7**. Note that the $|k_{ini}|$ values were calculated for each repeat separately, and subsequently averaged to obtain a good estimate of the error. When the rate of transport is low (< 10^{-3} s^{-1}), the relative error on the $|k_{ini}|$ values is high because transport is hardly detectable. The most accurate initial rates of transport are obtained for rates in the order of magnitude of 10^{-2} s^{-1} and 10^{-3} s^{-1}. Slow membrane crossing of iodide is also observable without transporter, as shown in **Figure S16** and **Table S8**. Bar graphs of the initial rate of transport are given in **Figure S17**-**Figure S21**.

It is clear that compound **1** does not transport any of the halide anions (the change in F/F_0 observed for iodide is due to unassisted permeation of iodide, comparable to the blank DMF run). Compounds **3** and **4** show fast transport of chloride, bromide and iodide and are therefore not selective transporters. The anion transport mediated by **3** and **4** is so fast that asymptotic fits could not be used and $|k_{ini}|$ had to be calculated via a linear fit of the first three data points, resulting in an underestimate of the anion transport rates and larger errors. Compound **2** and **5** are selective iodide transporters, with higher rates of iodide transport observed for **2** than for **5**, and they are therefore suitable for use in the TLF approach.

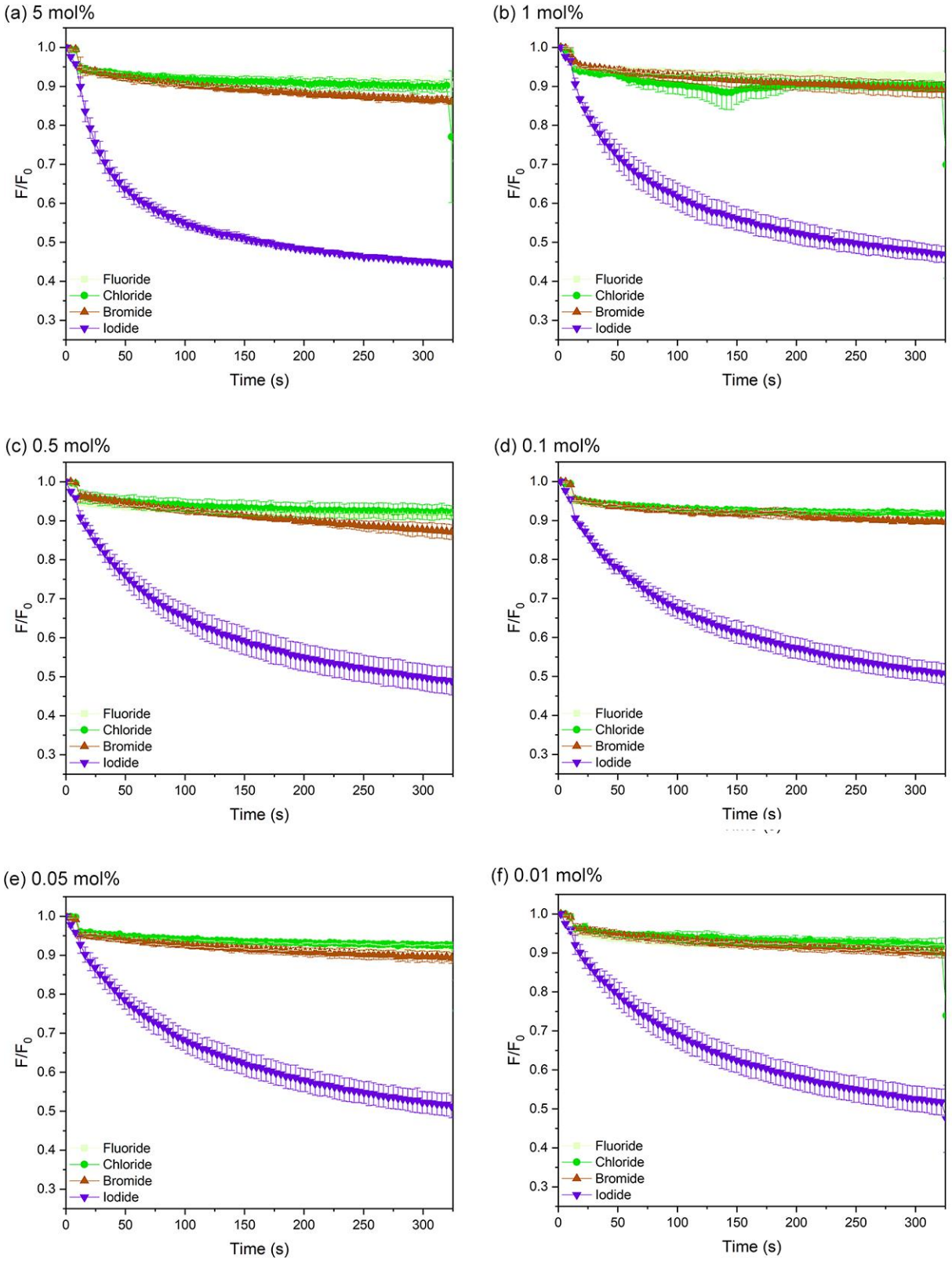

Figure S11. Kinetic anion transport traces of various concentrations of compound **1.** Experiment was performed as described in Section S5, and is the average of a minimum of 3 repeats (error bars represent standard deviations). (a) 5 mol% **1**, (b) 1 mol% **1**, (c) 0.5 mol% **1**, (d) 0.1 mol% **1**, (e) 0.05 mol% **1**, (f) 0.01 mol% **1**.

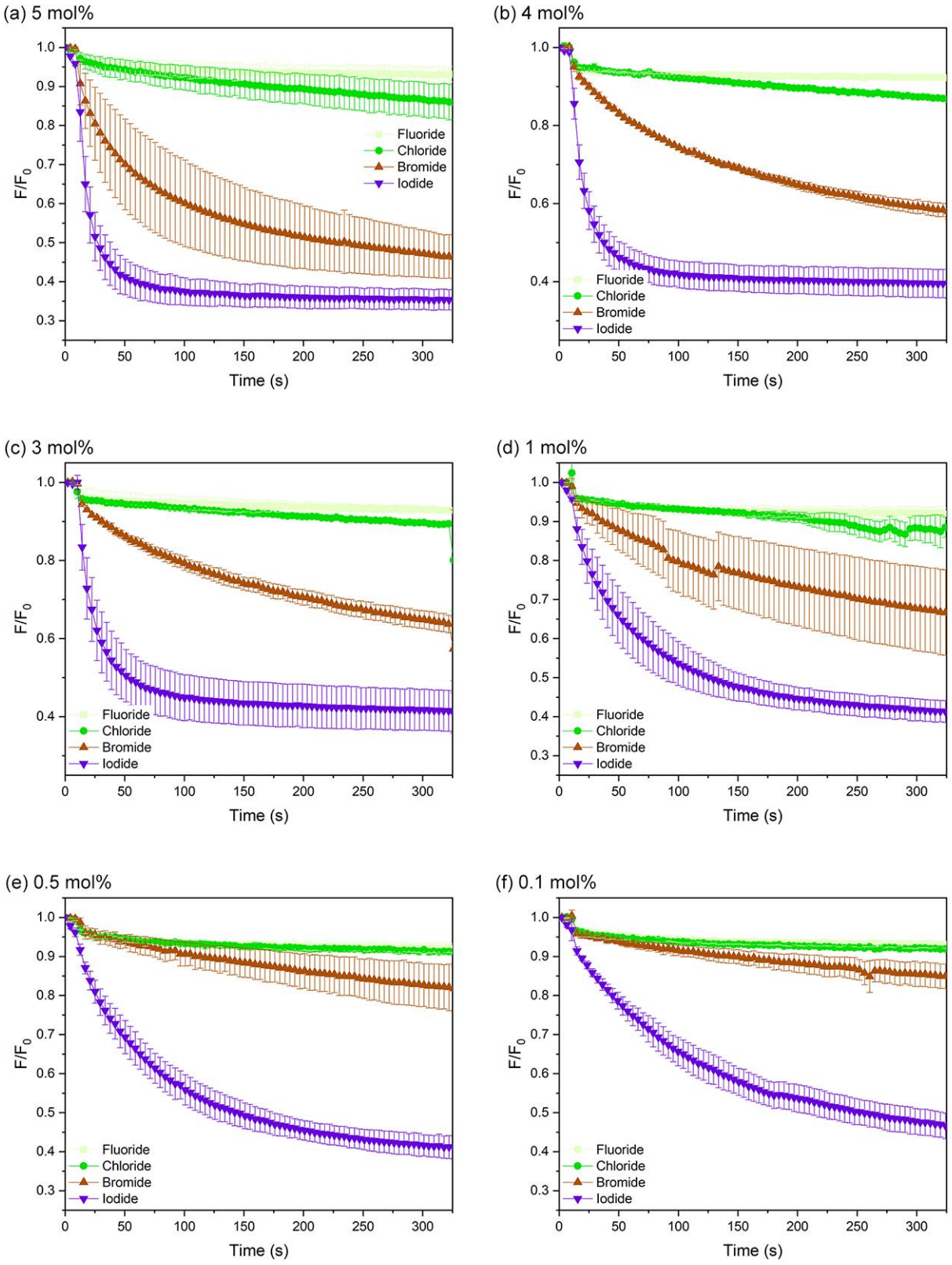

Figure S12. Kinetic anion transport traces of various concentrations of compound **2.** Experiment was performed as described in Section S5, and is the average of a minimum of 3 repeats (error bars represent standard deviations). (a) 5 mol% **2**, (b) 4 mol% **2**, (c) 3 mol% **2**, (d) 1 mol% **2**, (e) 0.5 mol% **2**, (f) 0.1 mol% **2**.

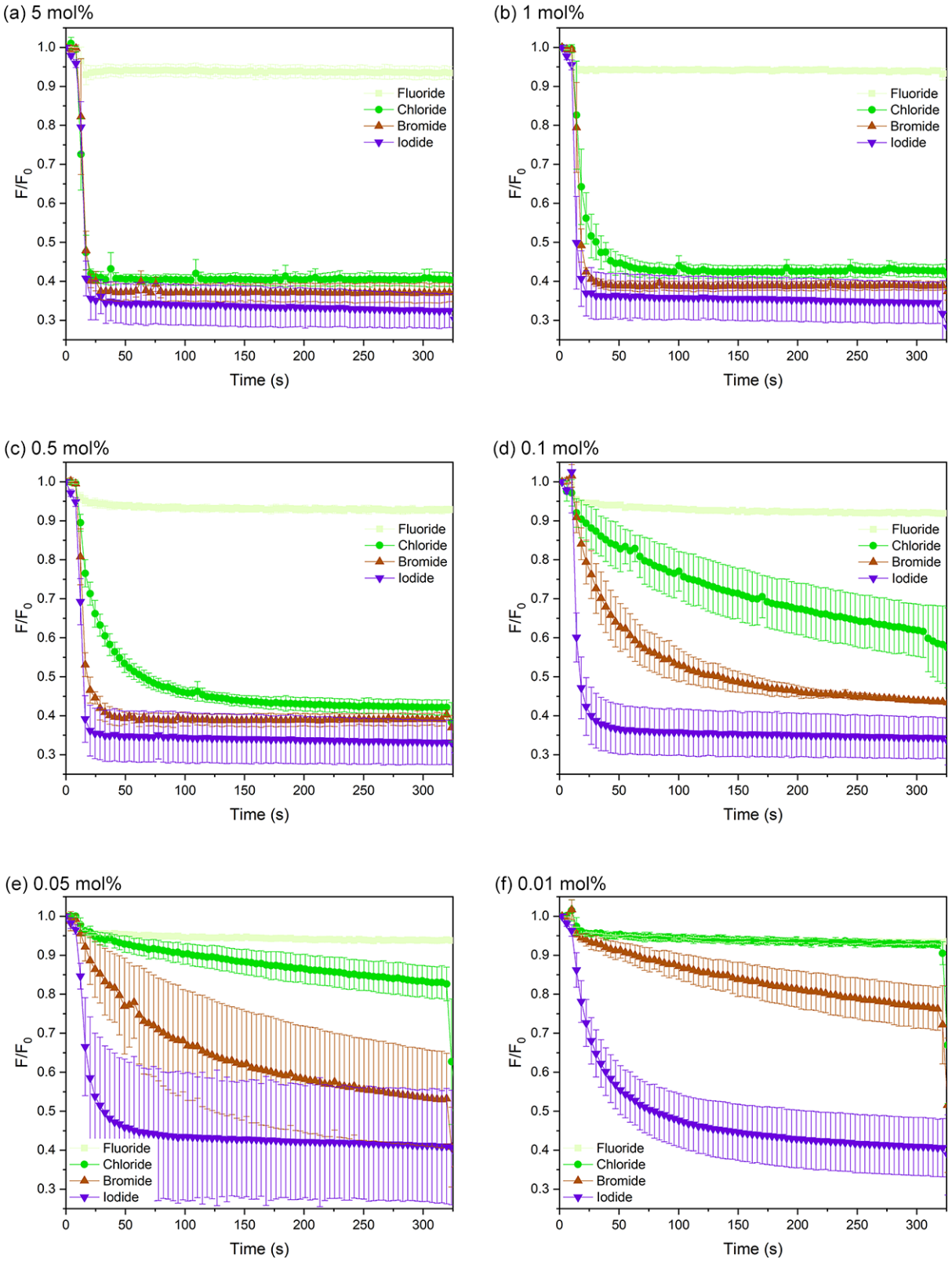

Figure S13. Kinetic anion transport traces of various concentrations of compound **3.** Experiment was performed as described in Section S5, and is the average of a minimum of 3 repeats (error bars represent standard deviations). (a) 5 mol% **3**, (b) 1 mol% **3**, (c) 0.5 mol% **3**, (d) 0.1 mol% **3**, (e) 0.05 mol% **3**, (f) 0.01 mol% **3**.

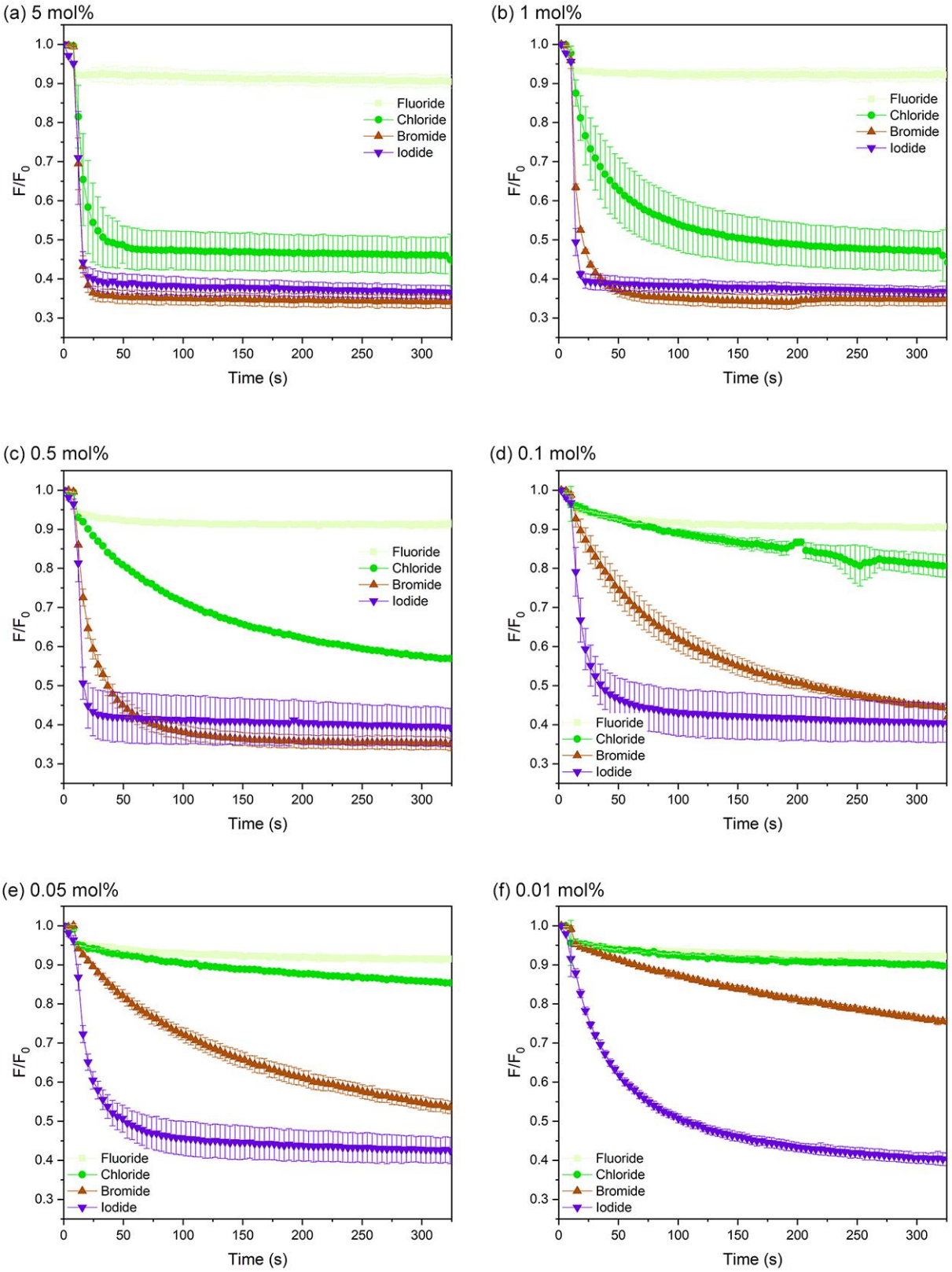

Figure S14. Kinetic anion transport traces of various concentrations of compound **4.** Experiment was performed as described in Section S5, and is the average of a minimum of 3 repeats (error bars represent standard deviations). (a) 5 mol% **4**, (b) 1 mol% **4**, (c) 0.5 mol% **4**, (d) 0.1 mol% **4**, (e) 0.05 mol% **4**, (f) 0.01 mol% **4**.

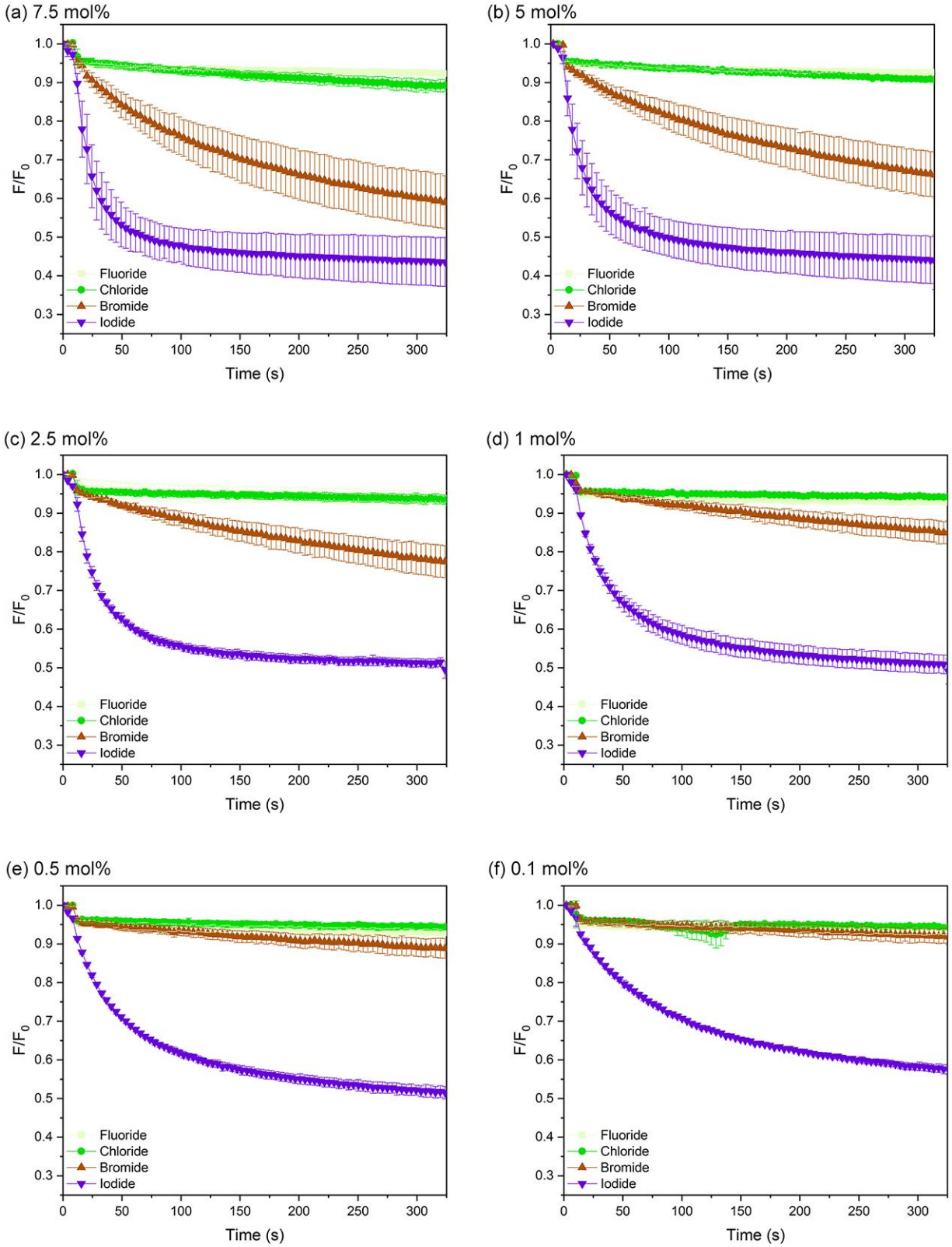

Figure S15. Kinetic anion transport traces of various concentrations of compound **5.** Experiment was performed as described in Section S5, and is the average of a minimum of 3 repeats (error bars represent standard deviations). (a) 7.5 mol% **5**, (b) 5 mol% **5**, (c) 2.5 mol% **5**, (d) 1 mol% **5**, (e) 0.5 mol% **5**, (f) 0.1 mol% **5**.

Table S3. Absolute initial rate of transport ($|k_{ini}|$) obtained for halide transport mediated by various concentration of compound **1**. Values are the average of minimum 3 independent repeats. Errors represent standard deviations.

Concentration	$\|k_{ini}\|$ for fluoride, s^{-1}	$\|k_{ini}\|$ for chloride s^{-1}	$\|k_{ini}\|$ for bromide s^{-1}	$\|k_{ini}\|$ for iodide s^{-1}
5 mol%	$(3.6 \pm 2.2)\cdot10^{-4}$	$(3.9 \pm 1.5)\cdot10^{-4}$	$(5.2 \pm 1.7)\cdot10^{-4}$	$(7.2 \pm 1.1)\cdot10^{-3}$
1 mol%	$(2.1 \pm 1.3)\cdot10^{-4}$	$(3.7 \pm 1.3)\cdot10^{-4}$	$(4.0 \pm 2.5)\cdot10^{-4}$	$(3.4 \pm 2.3)\cdot10^{-3}$
0.5 mol%	$(3.5 \pm 0.4)\cdot10^{-4}$	$(3.7 \pm 2.2)\cdot10^{-4}$	$(4.8 \pm 0.6)\cdot10^{-4}$	$(4.1 \pm 0.5)\cdot10^{-3}$
0.1 mol%	$(4.2 \pm 0.6)\cdot10^{-4}$	$(4.0 \pm 1.4)\cdot10^{-4}$	$(3.5 \pm 0.8)\cdot10^{-4}$	$(1.1 \pm 1.5)\cdot10^{-3}$
0.05 mol%	$(4.2 \pm 1.1)\cdot10^{-4}$	$(2.9 \pm 1.6)\cdot10^{-4}$	$(3.5 \pm 0.5)\cdot10^{-4}$	$(3.6 \pm 0.2)\cdot10^{-3}$
0.01 mol%	$(5.1 \pm 0.7)\cdot10^{-4}$	$(4.2 \pm 2.3)\cdot10^{-4}$	$(3.9 \pm 1.0)\cdot10^{-4}$	$(1.1 \pm 1.5)\cdot10^{-3}$

Table S4. Absolute initial rate of transport ($|k_{ini}|$) obtained for halide transport mediated by various concentration of compound **2**. Values are the average of minimum 3 independent repeats. Errors represent standard deviations.

Concentration	$\|k_{ini}\|$ for fluoride, s^{-1}	$\|k_{ini}\|$ for chloride s^{-1}	$\|k_{ini}\|$ for bromide s^{-1}	$\|k_{ini}\|$ for iodide s^{-1}
5 mol%	$(4.3 \pm 1.1)\cdot10^{-4}$	$(5.0 \pm 1.8)\cdot10^{-4}$	$(6.4 \pm 2.7)\cdot10^{-3}$	$(5.5 \pm 0.7)\cdot10^{-2}$
4 mol%	$(1.6 \pm 0.4)\cdot10^{-4}$	$(3.5 \pm 0.1)\cdot10^{-4}$	$(2.8 \pm 0.1)\cdot10^{-3}$	$(3.3 \pm 0.6)\cdot10^{-2}$
3 mol%	$(2.2 \pm 0.6)\cdot10^{-4}$	$(2.8 \pm 0.3)\cdot10^{-4}$	$(2.1 \pm 0.2)\cdot10^{-3}$	$(2.8 \pm 0.8)\cdot10^{-2}$
1 mol%	$(4.0 \pm 1.4)\cdot10^{-4}$	$(4.1 \pm 0.7)\cdot10^{-4}$	$(1.9 \pm 1.2)\cdot10^{-3}$	$(1.1 \pm 0.4)\cdot10^{-2}$
0.5 mol%	$(3.8 \pm 1.2)\cdot10^{-4}$	$(4.3 \pm 0.5)\cdot10^{-4}$	$(7.1 \pm 2.2)\cdot10^{-4}$	$(7.4 \pm 1.7)\cdot10^{-3}$
0.1 mol%	$(4.0 \pm 2.0)\cdot10^{-4}$	$(4.2 \pm 1.0)\cdot10^{-4}$	$(5.3 \pm 1.2)\cdot10^{-4}$	$(5.0 \pm 0.9)\cdot10^{-3}$

Table S5. Absolute initial rate of transport ($|k_{ini}|$) obtained for halide transport mediated by various concentration of compound **3**. Values are the average of minimum 3 independent repeats. Errors represent standard deviations.

Concentration	$\|k_{ini}\|$ for fluoride, s^{-1}	$\|k_{ini}\|$ for chloride s^{-1}	$\|k_{ini}\|$ for bromide s^{-1}	$\|k_{ini}\|$ for iodide s^{-1}
5 mol%	$(2.4 \pm 0.7)\cdot10^{-5}$	$(7.5 \pm 0.6)\cdot10^{-2}$	$(9.1 \pm 1.0)\cdot10^{-2}$	$(9.7 \pm 1.9)\cdot10^{-2}$
1 mol%	$(1.2 \pm 0.9)\cdot10^{-5}$	$(5.7 \pm 1.6)\cdot10^{-2}$	$(7.8 \pm 1.0)\cdot10^{-2}$	$(8.9 \pm 1.9)\cdot10^{-2}$
0.5 mol%	$(9.0 \pm 2.8)\cdot10^{-4}$	$(2.0 \pm 0.5)\cdot10^{-2}$	$(9.1 \pm 0.6)\cdot10^{-2}$	$(8.6 \pm 1.0)\cdot10^{-2}$
0.1 mol%	$(4.1 \pm 0.5)\cdot10^{-4}$	$(2.2 \pm 0.5)\cdot10^{-3}$	$(1.0 \pm 0.4)\cdot10^{-2}$	$(6.0 \pm 0.9)\cdot10^{-2}$
0.05 mol%	$(1.6 \pm 0.6)\cdot10^{-4}$	$(6.3 \pm 2.5)\cdot10^{-4}$	$(5.2 \pm 2.3)\cdot10^{-3}$	$(4.2 \pm 0.8)\cdot10^{-2}$
0.01 mol%	$(2.2 \pm 0.8)\cdot10^{-4}$	$(2.3 \pm 1.2)\cdot10^{-4}$	$(1.1 \pm 0.3)\cdot10^{-3}$	$(1.4 \pm 0.2)\cdot10^{-2}$

Table S6. Absolute initial rate of transport ($|k_{ini}|$) obtained for halide transport mediated by various concentration of compound **4**. Values are the average of minimum 3 independent repeats. Errors represent standard deviations.

Concentration	$\|k_{ini}\|$ for fluoride, s^{-1}	$\|k_{ini}\|$ for chloride s^{-1}	$\|k_{ini}\|$ for bromide s^{-1}	$\|k_{ini}\|$ for iodide s^{-1}
5 mol%	$(1.7 \pm 0.8)\cdot10^{-4}$	$(5.3 \pm 1.0)\cdot10^{-2}$	$(8.0 \pm 0.4)\cdot10^{-2}$	$(7.8 \pm 1.3)\cdot10^{-2}$
1 mol%	$(3.0 \pm 1.7)\cdot10^{-4}$	$(1.5 \pm 0.7)\cdot10^{-2}$	$(4.0 \pm 0.2)\cdot10^{-2}$	$(7.8 \pm 1.6)\cdot10^{-2}$
0.5 mol%	$(7.9 \pm 2.6)\cdot10^{-4}$	$(3.6 \pm 0.1)\cdot10^{-3}$	$(3.0 \pm 0.4)\cdot10^{-2}$	$(8.0 \pm 1.3)\cdot10^{-2}$
0.1 mol%	$(7.2 \pm 1.6)\cdot10^{-4}$	$(1.0 \pm 0.2)\cdot10^{-3}$	$(5.6 \pm 0.4)\cdot10^{-3}$	$(5.8 \pm 1.3)\cdot10^{-2}$
0.05 mol%	$(4.8 \pm 1.2)\cdot10^{-4}$	$(6.2 \pm 0.4)\cdot10^{-4}$	$(3.2 \pm 0.3)\cdot10^{-3}$	$(3.3 \pm 0.5)\cdot10^{-2}$
0.01 mol%	$(3.8 \pm 0.8)\cdot10^{-4}$	$(5.3 \pm 1.5)\cdot10^{-4}$	$(1.0 \pm 0.1)\cdot10^{-3}$	$(1.0 \pm 0.1)\cdot10^{-2}$

Table S7. Absolute initial rate of transport ($|k_{ini}|$) obtained for halide transport mediated by various concentration of compound **5**. Values are the average of minimum 3 independent repeats. Errors represent standard deviations.

Concentration	$\|k_{ini}\|$ for fluoride, s^{-1}	$\|k_{ini}\|$ for chloride s^{-1}	$\|k_{ini}\|$ for bromide s^{-1}	$\|k_{ini}\|$ for iodide s^{-1}
7.5 mol%	$(1.6\pm 0.1)\cdot10^{-4}$	$(2.9 \pm 0.2)\cdot10^{-4}$	$(2.7 \pm 0.7)\cdot10^{-3}$	$(2.9 \pm 1.0)\cdot10^{-2}$
5 mol%	$(1.5 \pm 0.5)\cdot10^{-4}$	$(2.0 \pm 0.5)\cdot10^{-4}$	$(1.7 \pm 0.5)\cdot10^{-3}$	$(2.3 \pm 0.6)\cdot10^{-2}$
2.5 mol%	$(1.6 \pm 0.5)\cdot10^{-4}$	$(8.5 \pm 3.5)\cdot10^{-5}$	$(8.8 \pm 2.6)\cdot10^{-4}$	$(1.6 \pm 0.2)\cdot10^{-2}$
1 mol%	$(1.5 \pm 0.6)\cdot10^{-4}$	$(8.9 \pm 1.5)\cdot10^{-5}$	$(4.6 \pm 1.4)\cdot10^{-4}$	$(1.2 \pm 0.2)\cdot10^{-2}$
0.5 mol%	$(1.6 \pm 0.2)\cdot10^{-4}$	$(1.2 \pm 0.3)\cdot10^{-4}$	$(2.9 \pm 0.8)\cdot10^{-4}$	$(7.0 \pm 0.6)\cdot10^{-3}$
0.1 mol%	$(1.2 \pm 0.4)\cdot10^{-4}$	$(1.4 \pm 0.5)\cdot10^{-4}$	$(1.6 \pm 0.5)\cdot10^{-4}$	$(3.8 \pm 0.4)\cdot10^{-3}$

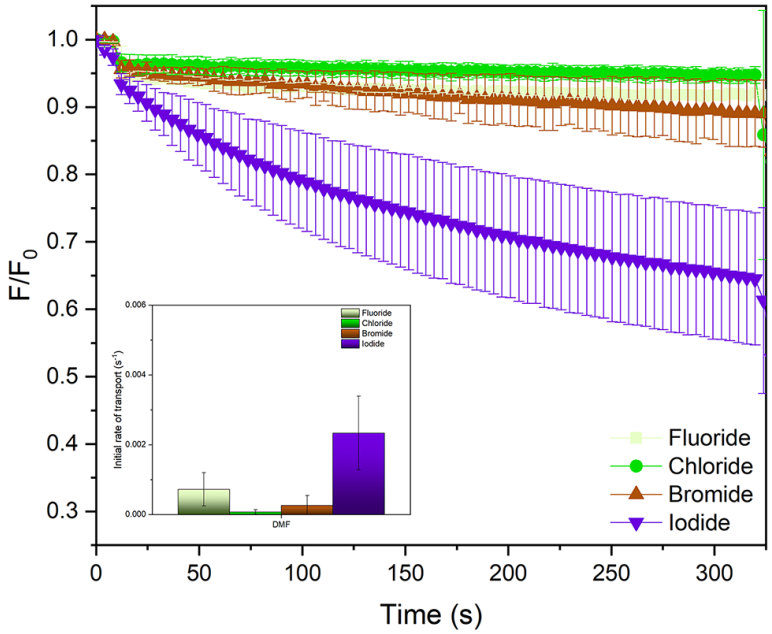

Figure S16. Kinetic anion transport traces in the absence of transporter (DMF was added at time t = 10 s). Experiment was performed as described in Section S5, and is the average of a minimum of 3 repeats (error bars represent standard deviations). Insets shows the bar graph of the obtained initial rate of transport for each anion

Table S8. Absolute initial rate of transport ($|k_{ini}|$) obtained in the absence of transporter. Values are the average of minimum 3 independent repeats. Errors represent standard deviations.

Halide	$\|k_{ini}\|$, s^{-1}
fluoride	$(7.3\pm 4.7)\cdot10^{-4}$
chloride	$(7.2\pm 6.7)\cdot10^{-5}$
bromide	$(2.7\pm 2.8)\cdot10^{-4}$
iodide	$(2.3 \pm 1.1)\cdot10^{-3}$

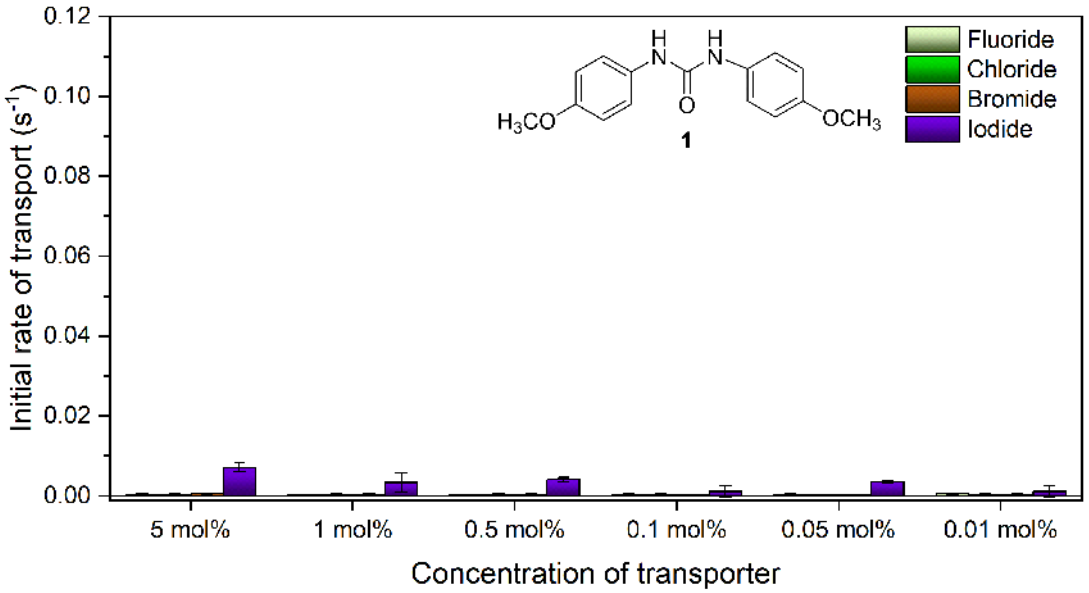

Figure S17. Halide sensing by the TLF systems based on lucigenin, eggPC liposomes and various concentrations of transporter **1**. Concentrations of transporter are given as mol% with respect to EggPC lipid concentration. Experiments and data analysis were performed as described in Section S5. Results are the average of minimum 3 independent repeats and errors bars represent standard deviations.

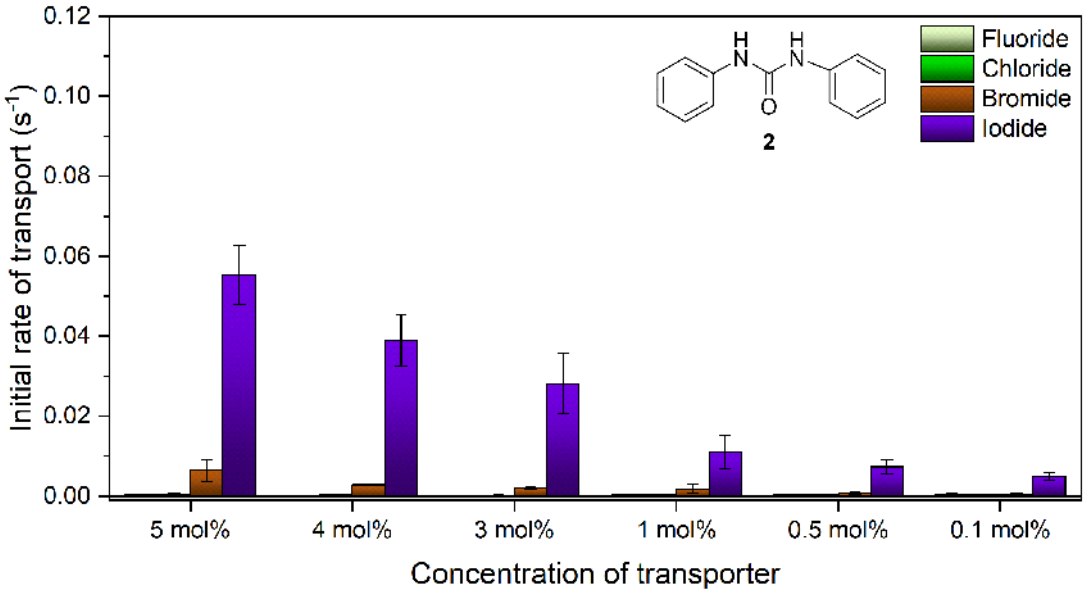

Figure S18. Halide sensing by the TLF systems based on lucigenin, eggPC liposomes and various concentrations of transporter **2**. Concentrations of transporter are given as mol% with respect to EggPC lipid concentration. Experiments and data analysis were performed as described in Section S5. Results are the average of minimum 3 independent repeats and errors bars represent standard deviations.

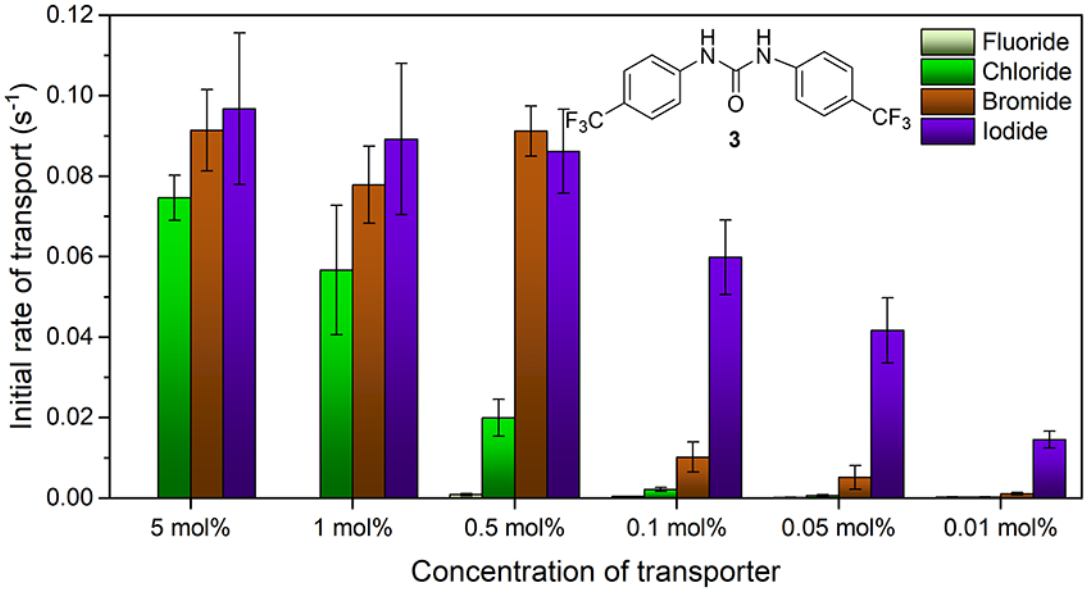

Figure S19. Halide sensing by the TLF systems based on lucigenin, eggPC liposomes and various concentrations of transporter **3**. Concentrations of transporter are given as mol% with respect to EggPC lipid concentration. Experiments and data analysis were performed as described in Section S5. Results are the average of minimum 3 independent repeats and errors bars represent standard deviations.

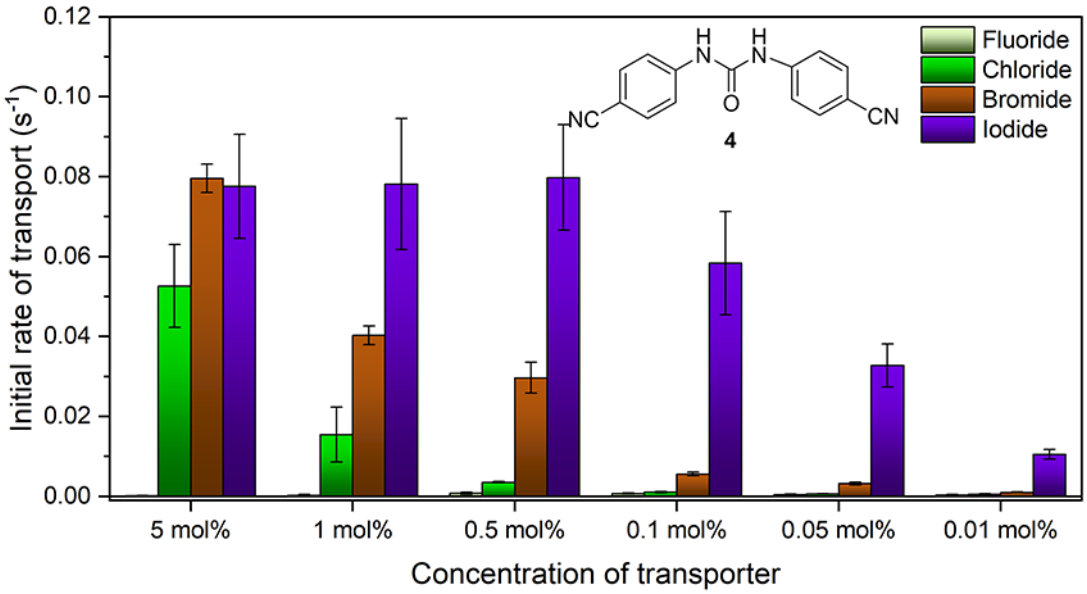

Figure S20. Halide sensing by the TLF systems based on lucigenin, eggPC liposomes and various concentrations of transporter **4**. Concentrations of transporter are given as mol% with respect to EggPC lipid concentration. Experiments and data analysis were performed as described in Section S5. Results are the average of minimum 3 independent repeats and errors bars represent standard deviations.

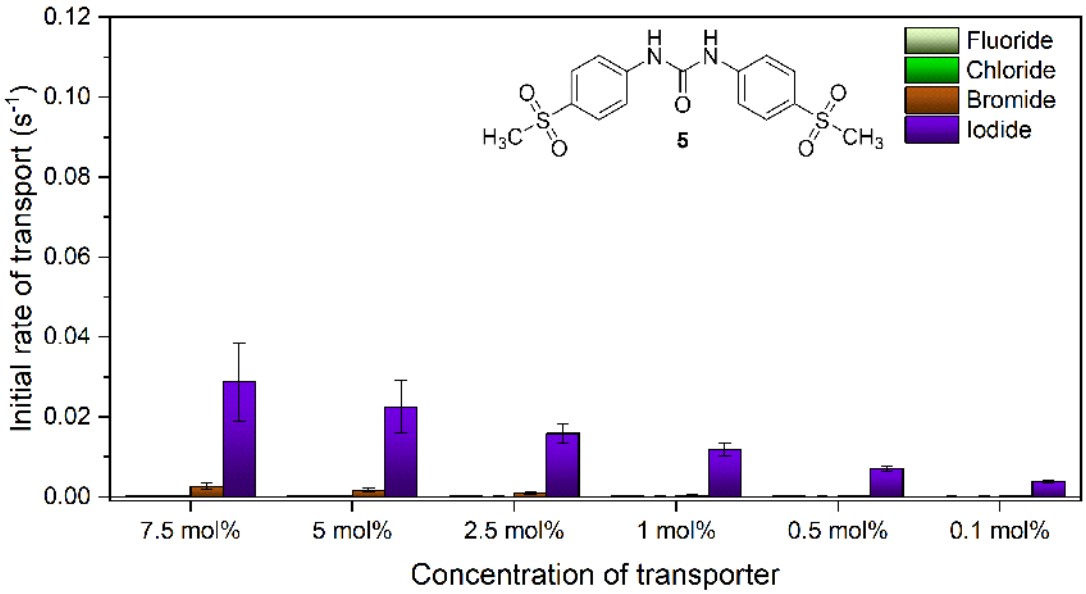

Figure S21. Halide sensing by the TLF systems based on lucigenin, eggPC liposomes and various concentrations of transporter **5**. Concentrations of transporter are given as mol% with respect to EggPC lipid concentration. Experiments and data analysis were performed as described in Section S5. Results are the average of minimum 3 independent repeats and errors bars represent standard deviations.

S7. Determination of the detection limit and dynamic range of the TLF systems

S7.1. Dynamic range of parent lucigenin

To a solution of 0.25 µM lucigenin in nitrate buffer (222 mM $NaNO_3$, 5 mM HEPES, pH 7.4) was added sodium iodide at various concentrations. The fluorescence spectrum (excitation 430 nm) was measured before and after addition of the salt. The spectra were normalized by dividing the fluorescence intensity at any wavelength by the fluorescence intensity at 505 nm before the addition of salt (**Figure S22**). The experiment was repeated 3 times. The percent of fluorescence quenching was calculated using the fluorescence intensity at 505 nm (F_{505nm}). The graph of the % quenching versus iodide concentration is shown in **Figure S23**, which clearly shows an upper limit for iodide concentrations that can be determined. The major change takes place in the region 0.75-25 mM NaI, after which the curve flattens out and determination of iodide concentration becomes less reliable.

$$\%\ quenching = \left(1 - \frac{F_{505nm}\ after\ addition\ salt}{F_{505nm}\ before\ addition\ salt}\right) \cdot 100\%$$

For the Stern-Volmer constant, the F_0/F value at 505 nm was calculated and plotted against the iodide concentration (**Figure S24**). The Stern-Volmer constant, K_{SV}, is given by the slope of the linear fit. Although a linear fit with good R^2 value can be obtained for the full range (0.75-100 mM), it clearly shows a systematic error (**Figure S24, red line**). When a linear fit is performed for the range 0.75-25 mM (which shows the largest absolute change in fluorescence), the higher concentrations appear to deviate from this linearity (**Figure S24, black/dashed line**). Therefore, the dynamic range of lucigenin is 0.75 mM – 25 mM iodide and the determination of higher iodide concentrations should only be used with caution.

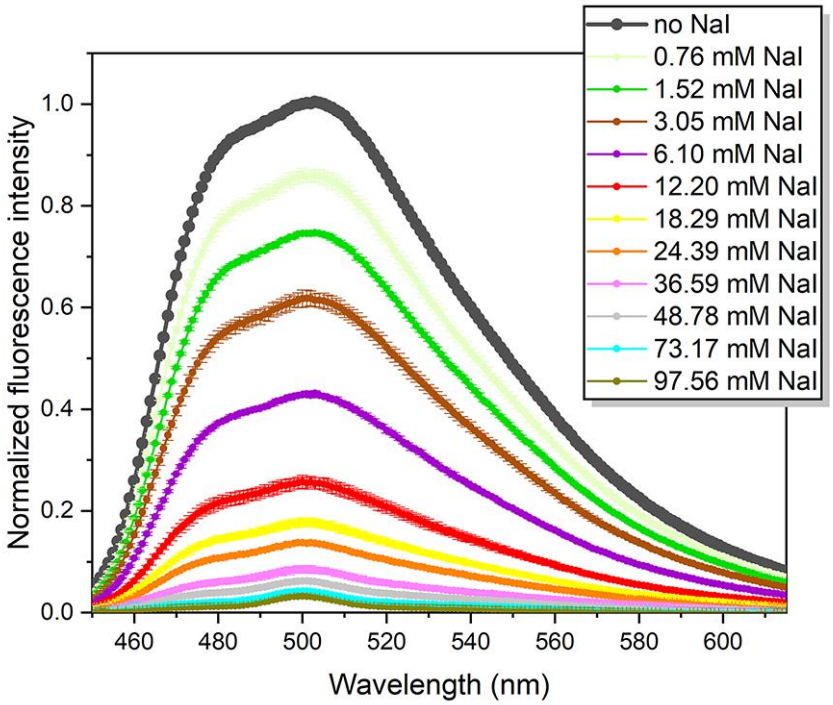

Figure S22. Normalized fluorescence spectra of lucigenin in the presence of various concentrations NaI. The excitation wavelength was 430 nm. Results are the average of 3 repeats and error bars represent standard deviations.

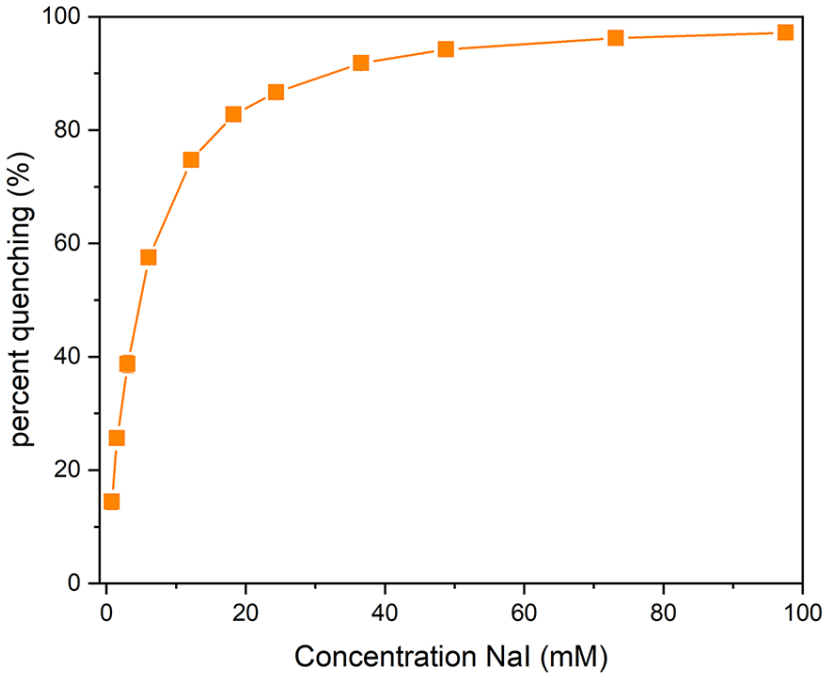

Figure S23. Relationship between the percent of lucigenin quenching by various concentrations of NaI. The excitation wavelength was 430 nm, and the emission was measured at 505 nm. Results are the average of 3 repeats and error bars represent standard deviations.

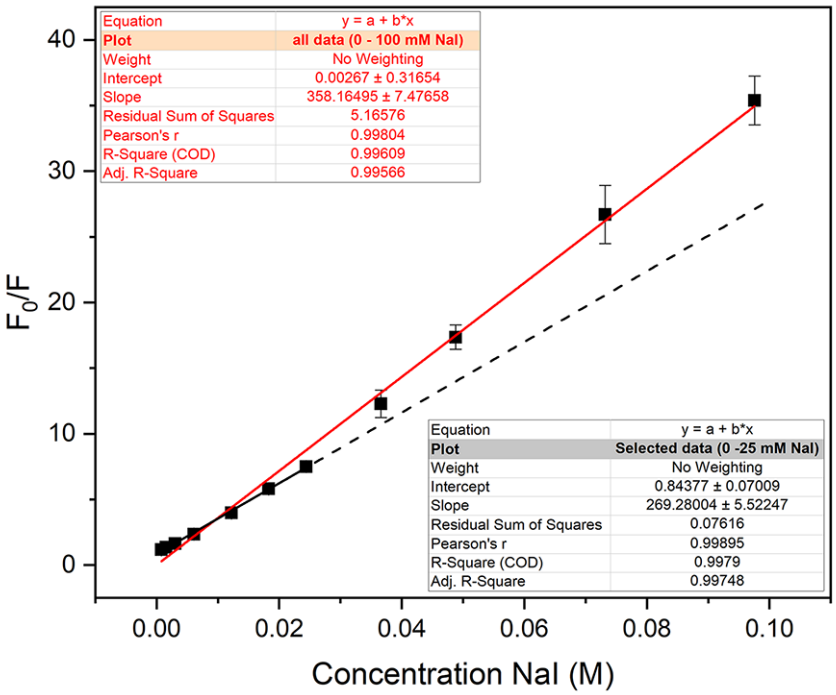

Figure S24. Stern-Volmer plot of the quenching of lucigenin by various concentrations NaI. Linear fits were performed for the range 0 – 0.1 M NaI (solid red line) and 0 – 0.025 M NaI (solid black line). Extrapolation of the linear fit on the smaller NaI concentration range indicates that determination of high NaI concentrations is not reliable (dashed black line).

*S7.2. Dynamic range of TLF system based on compounds **2** and **5***

To determine the dynamic range of the TLF system based on compounds **2** and **5**, the anion transport kinetic assay was performed as described in Section S5. However, NaI stock solutions with varying concentrations were used to achieve final concentrations of 24.4, 18.3, 12.2, 6.1, 3.0, 1.5 and 0.76 mM iodide. The initial rate of transport was calculated for all iodide concentrations, and a calibration curve of $|k_{ini}|$ vs iodide concentration was plotted. The data was linear fitted using OriginPro 2019, yielding good R^2-values > 0.96. The results are shown in **Figure S25 - Figure S28**. Note that the errors and R^2-values associated with the TLF system based on compound **5** are larger than for compound **2**. It is possible that the higher concentrations of compound **5** that are needed to achieve iodide transport lead to aggregation and therefore more varied results. The errors for the TLF system based on compound **2** are only large because the results are the average of 3 repeats run on different batches of liposomes to investigate the robustness of the system. However, when an unknown sample needs to be tested, a calibration would be performed on the same liposomes as the sample (see Section S9), yielding smaller errors.

For the best system, based on 4 mol% compound **2**, an extended calibration was performed with NaI concentrations up to 100 mM. A good linear fit is obtained at these high NaI concentrations, that does not show significant variation between a linear fit over the 0-25 mM NaI range and 0-100 mM NaI range (**Figure S29**). More data points were collected to obtain accurate initial rate of transport values ($|k_{ini}|$) for NaI concentration > 20 mM (data point every 0.05 seconds). All 3 repeats were performed on the same batch of liposomes. $|k_{ini}|$ values > 0.1 s^{-1} indicate very steep kinetic traces and are therefore less reliable. The upper limit for iodide detection by this TLF system is therefore 100 mM NaI.

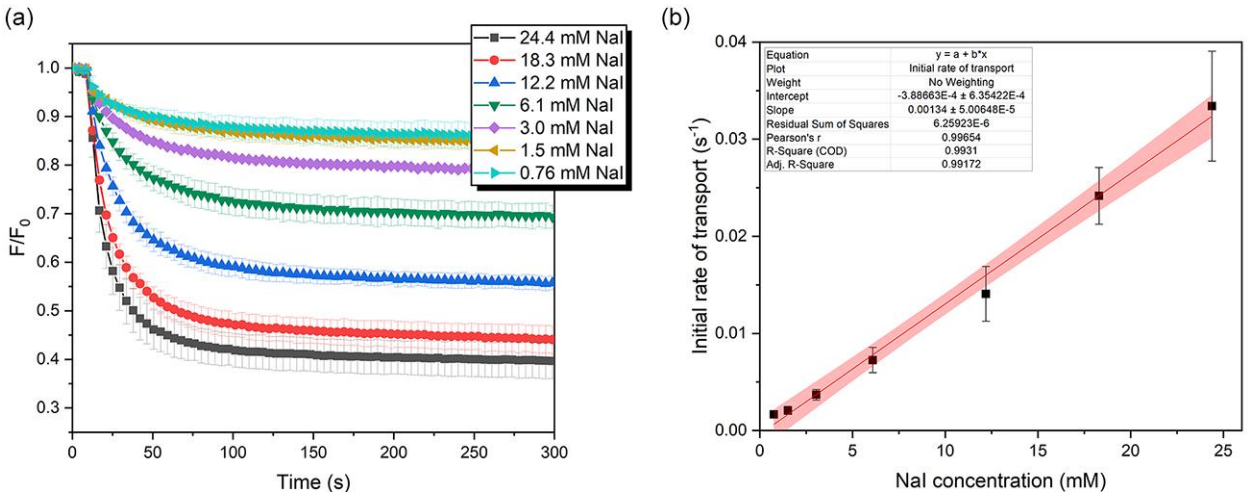

Figure S25. (a) Kinetic anion transport traces of the TLF system based on compound **2** (4 mol%) using various concentrations of NaI (0 – 25 mM)**.** Experiments were performed as described in Section S5, and are the average of a minimum of 3 repeats (error bars represent standard deviations). (b) Calibration curve showing the linear correlation between the NaI concentration and the obtained initial rate of transport for the TLF system based on compound **2** (4 mol%). Linear fit was performed using OriginPro 2019 without weighting. Red band shows 95% confidence interval.

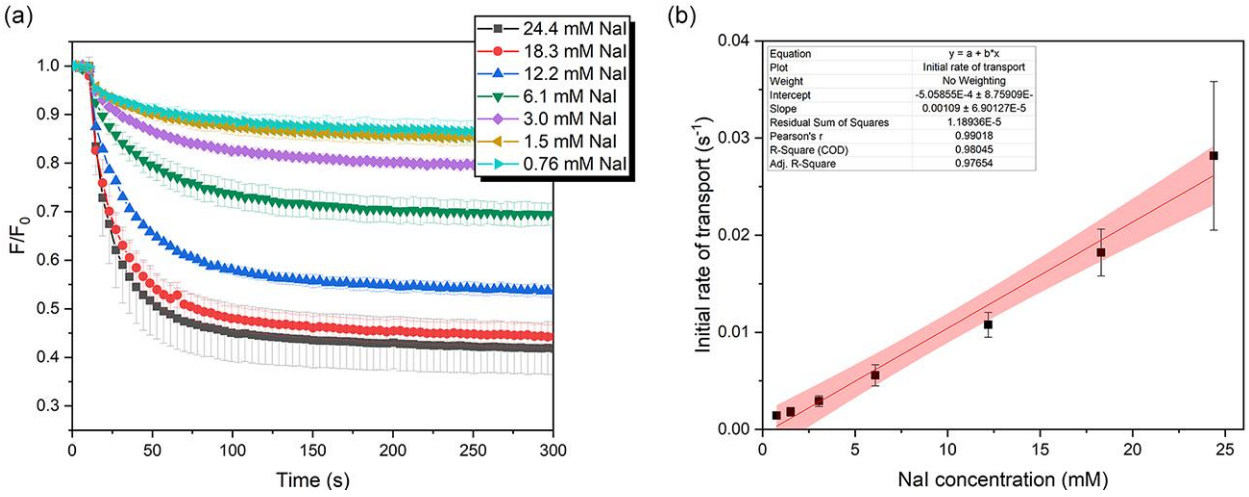

Figure S26. (a) Kinetic anion transport traces of the TLF system based on compound **2** (3 mol%) using various concentrations of NaI (0 -25 mM)**.** Experiments were performed as described in Section S5, and are the average of a minimum of 3 repeats (error bars represent standard deviations). (b) Calibration curve showing the linear correlation between the NaI concentration and the obtained initial rate of transport for the TLF system based on compound **2** (3 mol%). Linear fit was performed using OriginPro 2019 without weighting. Red band shows 95% confidence interval.

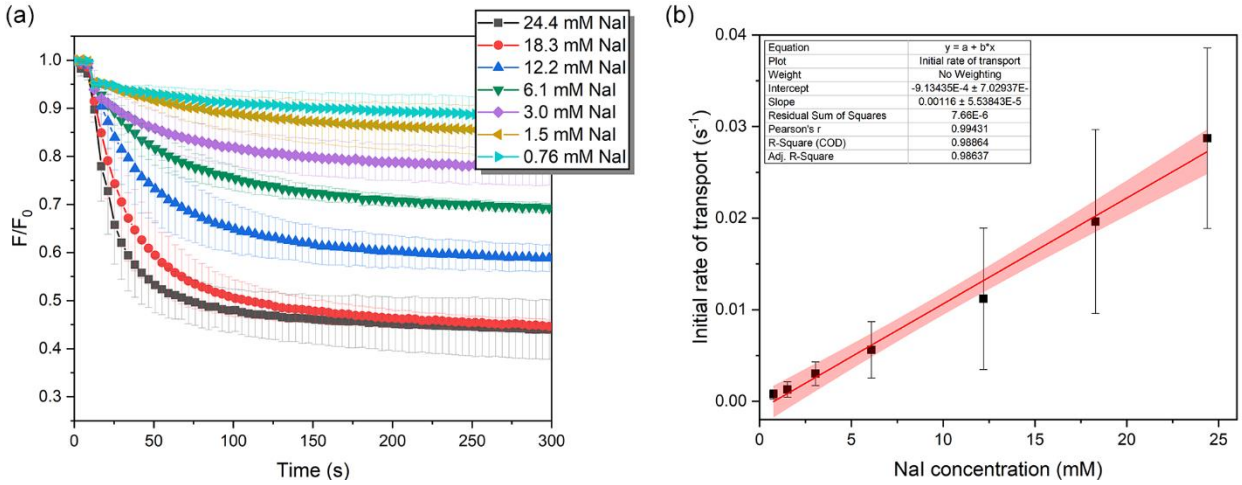

Figure S27. (a) Kinetic anion transport traces of the TLF system based on compound **5** (7.5 mol%) using various concentrations of NaI (0 – 25 mM)**.** Experiments were performed as described in Section S4, and are the average of a minimum of 3 repeats (error bars represent standard deviations). (b) Calibration curve showing the linear correlation between the NaI concentration and the obtained initial rate of transport for the TLF system based on compound **5** (7.5 mol%). Linear fit was performed using OriginPro 2019 without weighting. Red band shows 95% confidence interval.

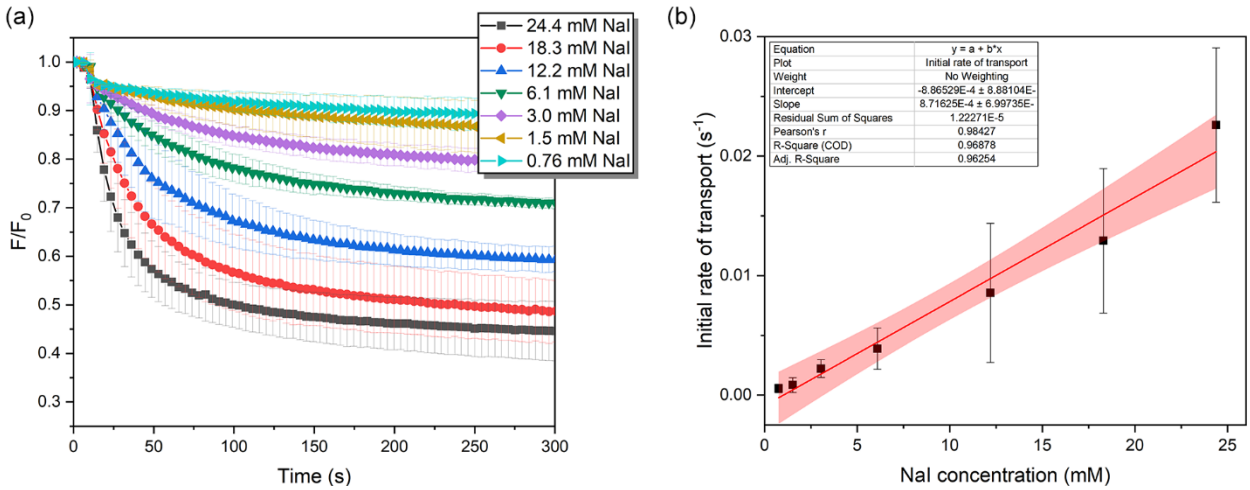

Figure S28. (a) Kinetic anion transport traces of the TLF system based on compound **5** (5 mol%) using various concentrations of NaI (0 – 25 mM)**.** Experiments were performed as described in Section S4, and are the average of a minimum of 3 repeats (error bars represent standard deviations). (b) Calibration curve showing the linear correlation between the NaI concentration and the obtained initial rate of transport for the TLF system based on compound **5** (5 mol%). Linear fit was performed using OriginPro 2019 without weighting. Red band shows 95% confidence interval.

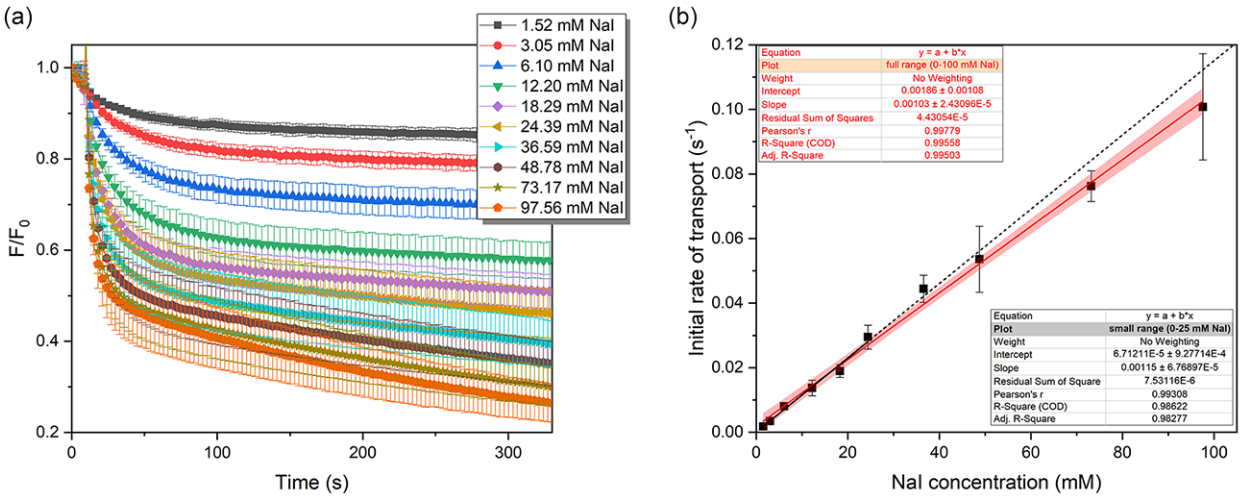

Figure S29. (a) Kinetic anion transport traces of the TLF system based on compound **2** (4 mol%) using various concentrations of NaI (0 – 100 mM)**.** Experiments were performed as described in Section S5, and are the average of a minimum of 3 repeats (error bars represent standard deviations). (b) Calibration curve showing the linear correlation between the NaI concentration and the obtained initial rate of transport for the TLF system based on compound **2** (4 mol%). Linear fit was performed using OriginPro 2019 without weighting. Red band shows 95% confidence interval.

S7.3. Dynamic range of TLF system without transporter (DMF)

To determine the dynamic range of the TLF system without transporter, the anion transport kinetic assay was performed as described in Section S5. However, NaI stock solutions with varying concentrations were used to achieve final concentrations between 0 – 100 mM iodide, and neat DMF was added instead of a transporter solution. The initial rate of transport was calculated for all iodide concentrations, and a calibration curve of $|k_{ini}|$ vs iodide concentration was plotted. The results are shown in **Figure S30** and **Figure S31**. While a linear fit can be performed for the range 0 – 40 mM NaI, it is clear that the relationship between spontaneous iodide permeation (without transporter) and iodide concentration is not linear (**Figure S30**). This is even more visible when only the data from a single repeat on the same batch of liposomes is plotted (**Figure S31**). This sigmoidal correlation therefore implies that the determination of iodide concentrations above 25 mM is not reliable due to flattening of the curve. Furthermore, low iodide concentrations (<5 mM) do not show a visible response of the system and the calculated initial rate of transport ($|k_{ini}|$ values) below this threshold is therefore the same with very large relative errors. In general, the errors at such low transmembrane rates are high. The dynamic range of the TLF system without transporter (5 - 40 mM iodide), is therefore considerably worse to the dynamic range of the TLF system based on 4 mol% compound **2** (0.75 – 100 mM iodide).

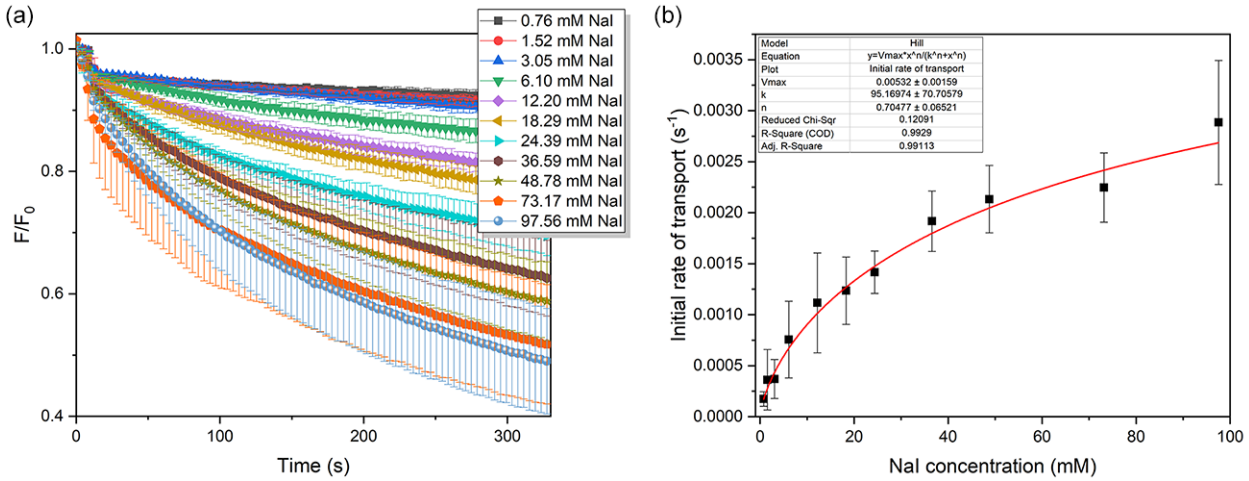

Figure S30. (a) Kinetic anion transport traces of the TLF system without transporter using various concentrations of NaI (0 – 100 mM)**.** Experiments were performed as described in Section S5, and are the average of a minimum of 5 repeats (error bars represent standard deviations). (b) Calibration curve showing the correlation between the NaI concentration and the obtained initial rate of transport for the TLF system without transporter. Sigmoidal fit was performed using OriginPro 2019 without weighting.

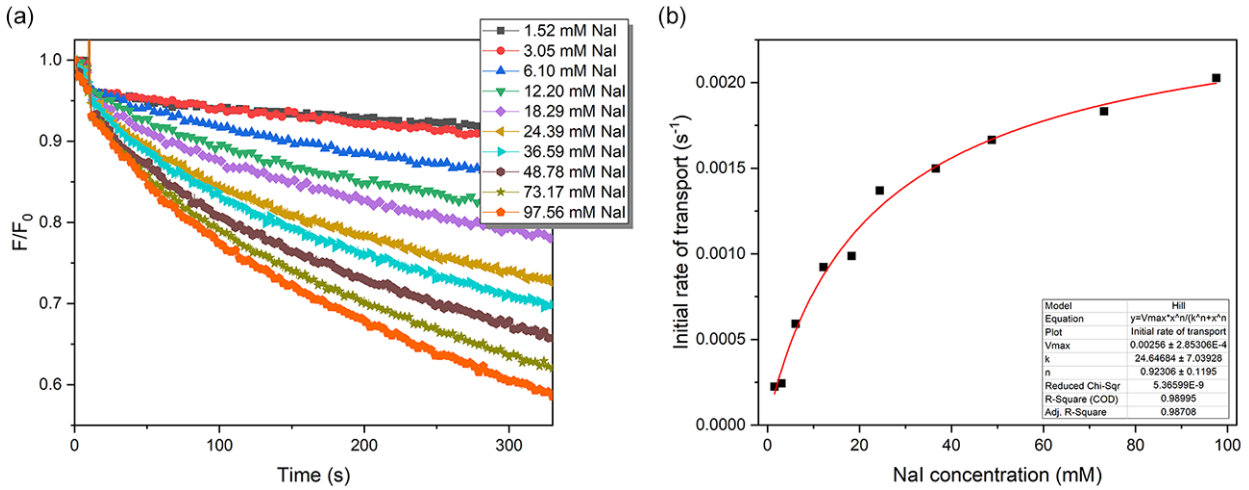

Figure S31. (a) Kinetic anion transport traces of the TLF system without transporter using various concentrations of NaI (0 – 100 mM)**.** Experiments were performed as described in Section S5, and are the result of 1 repeat performed on the same batch of liposomes. (b) Calibration curve showing the correlation between the NaI concentration and the obtained initial rate of transport for the TLF system without transporter. Sigmoidal fit was performed using OriginPro 2019 without weighting.

S8. Detection of iodide in the presence of excess chloride by the TLF systems

To determine the true functionality/selectivity of this TLF method for iodide sensing, we wanted to see if the iodide concentration can be accurately determined in the presence of another anion. Chloride was chosen as the other anion, because it is able to quench lucigenin and is commonly found

in nature and therefore a likely contaminant. Nine combinations of NaI solutions (24.4 mM, 12.2 mM, 2.4 mM) spiked with either 24.4 mM, 12.2 mM or 2.4 mM NaCl were made. The kinetic anion transport assay was performed and the initial rate of transport was calculated as described in Section S5. The obtained $|k_{ini}|$ values were used to predict the iodide concentration in the contaminated samples using the calibration curves found in Section S7. Predicted vs. actual NaI concentration plots that produce a linear fit with a slope close to 1 indicate that the NaCl contamination has no effect on the ability of the TLF system to determine iodide concentrations. The results are shown in **Figure S32 – Figure S46**. The best results are obtained for the TLF system based on compound **2**, which shows the fastest iodide transport and therefore produces calibration curves with a large slope which makes it more reliable. The result with compound **5** and without transporter, show much larger errors and thus a worse prediction.

*S8.1. Results for the TLF system based on 4 mol% compound **2***

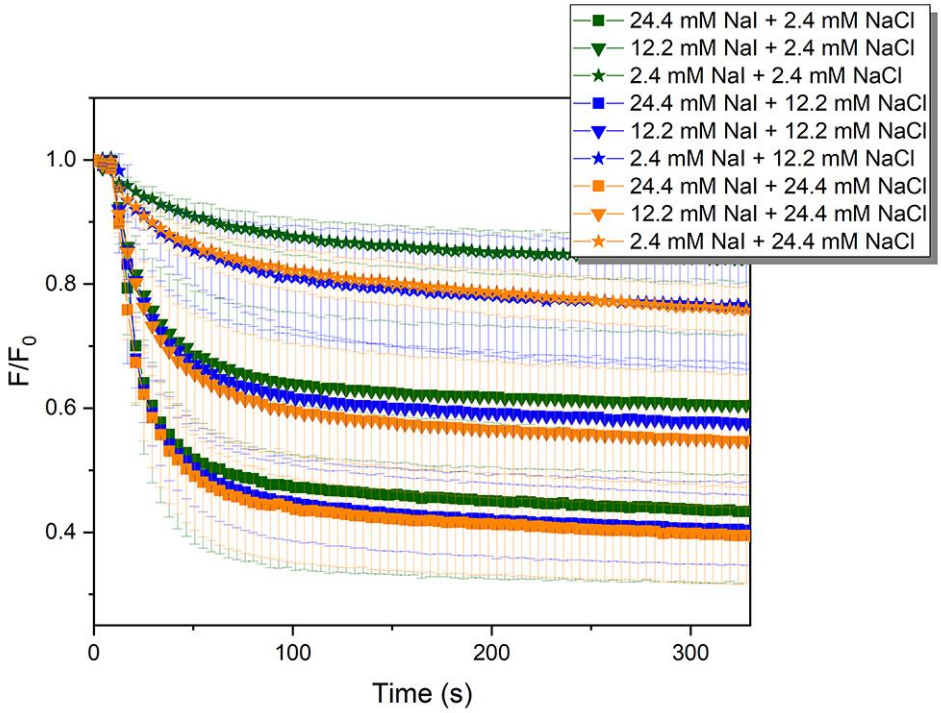

Figure S32. Kinetic anion transport traces of the TLF system based on 4 mol% compound **2**. Anion transport involved NaI sample (iodide transport) contaminated with 2.4 mM NaCl (dark green), 12.2 mM NaCl (blue) or 24.4 mM NaCl (orange). Experiments were performed as described in Section S5, and are the average of a minimum of 3 repeats (error bars represent standard deviations).

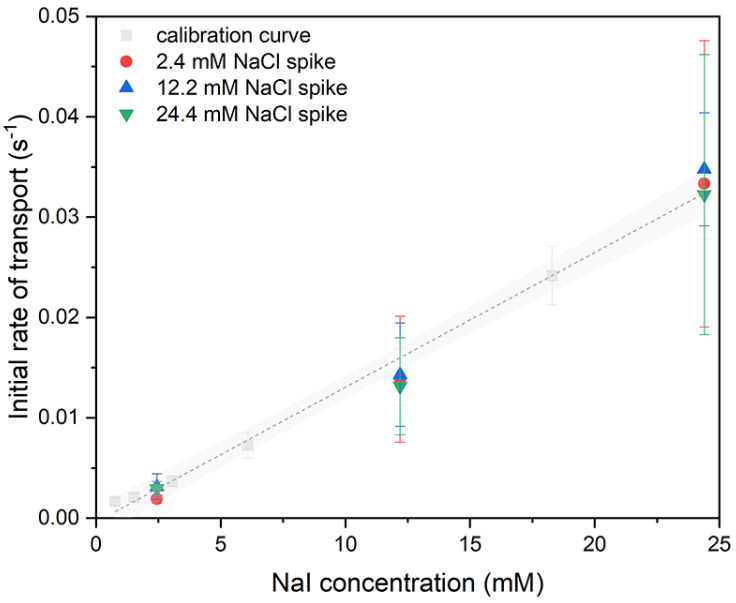

Figure S33. Initial rate of transport obtained from the kinetic anion transport traces shown in Figure S32 overlaid onto the NaI calibration curve for the TLF system based on 4 mol% compound **2** (Figure S25). Grey band shows the 95% confidence interval of the calibration curve.

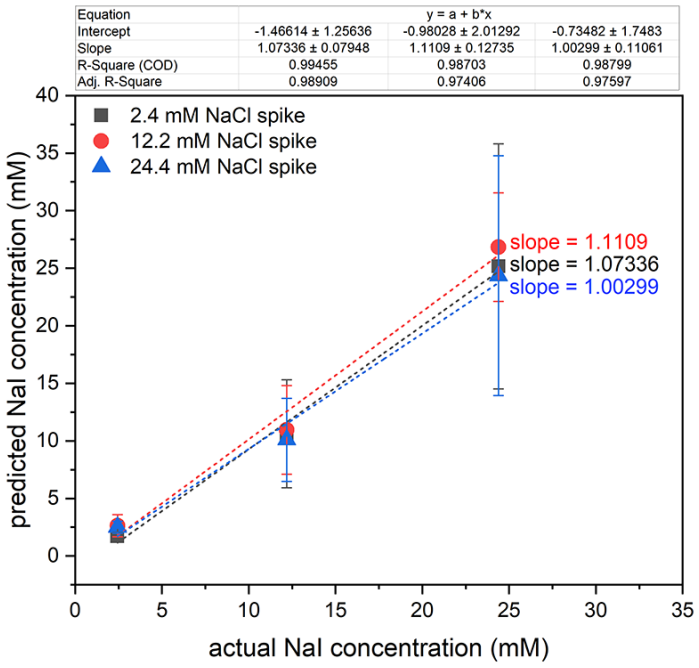

Figure S34. Predicted NaI concentrations (using the calibration curve of Figure S25) versus actual NaI concentration in the NaCl-contaminated samples.

*S8.2. Results for the TLF system based on 3 mol% compound **2***

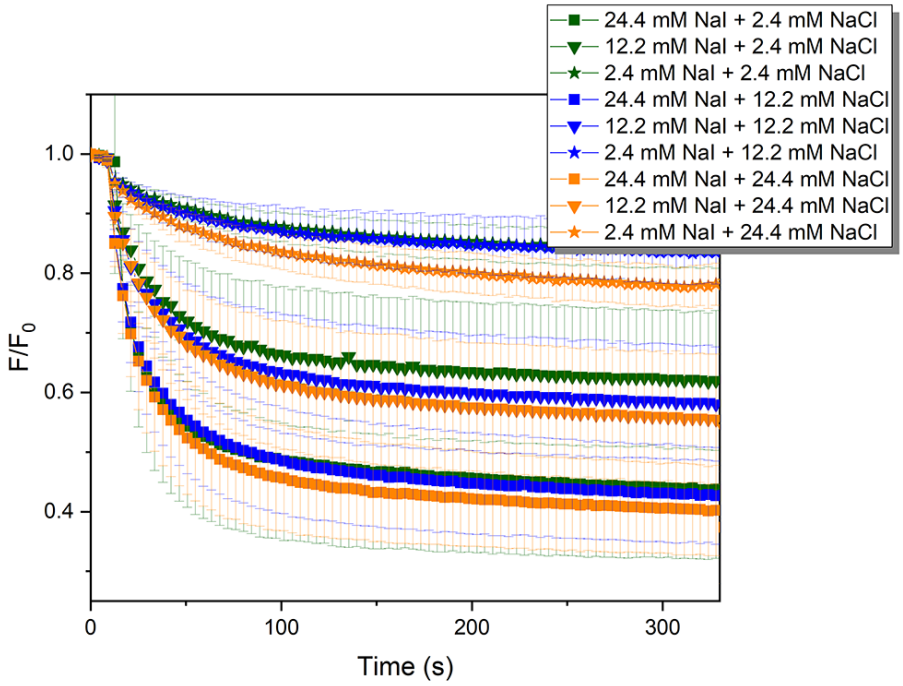

Figure S35. Kinetic anion transport traces of the TLF system based on 3 mol% compound **2**. Anion transport involved NaI sample (iodide transport) contaminated with 2.4 mM NaCl (dark green), 12.2 mM NaCl (blue) or 24.4 mM NaCl (orange). Experiments were performed as described in Section S5, and are the average of a minimum of 3 repeats (error bars represent standard deviations).

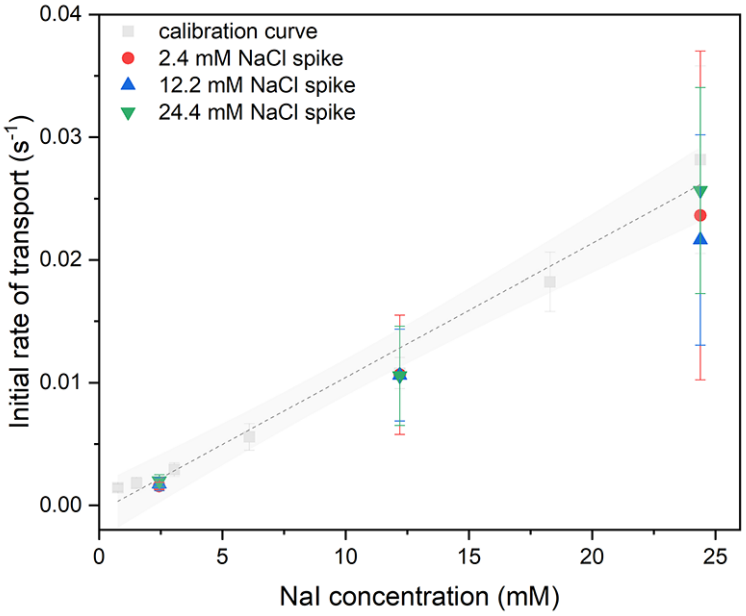

Figure S36. Initial rate of transport obtained from the kinetic anion transport traces shown in Figure S35 overlaid onto the NaI calibration curve for the TLF system based on 3 mol% compound **2** (Figure S26). Grey band shows the 95% confidence interval of the calibration curve.

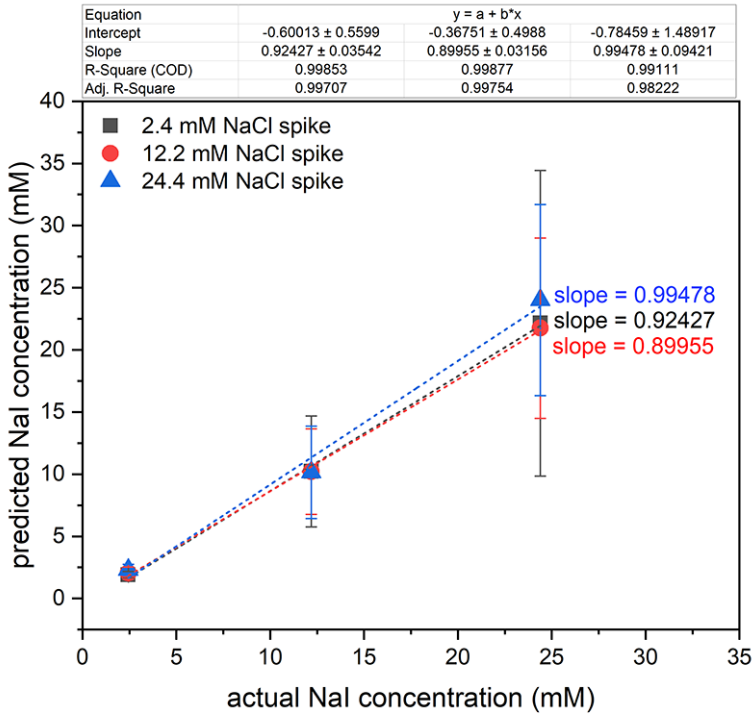

Figure S37. Predicted NaI concentrations (using the calibration curve of Figure 26) versus actual NaI concentration in the NaCl-contaminated samples.

*S8.3. Results for the TLF system based on 7.5 mol% compound **5***

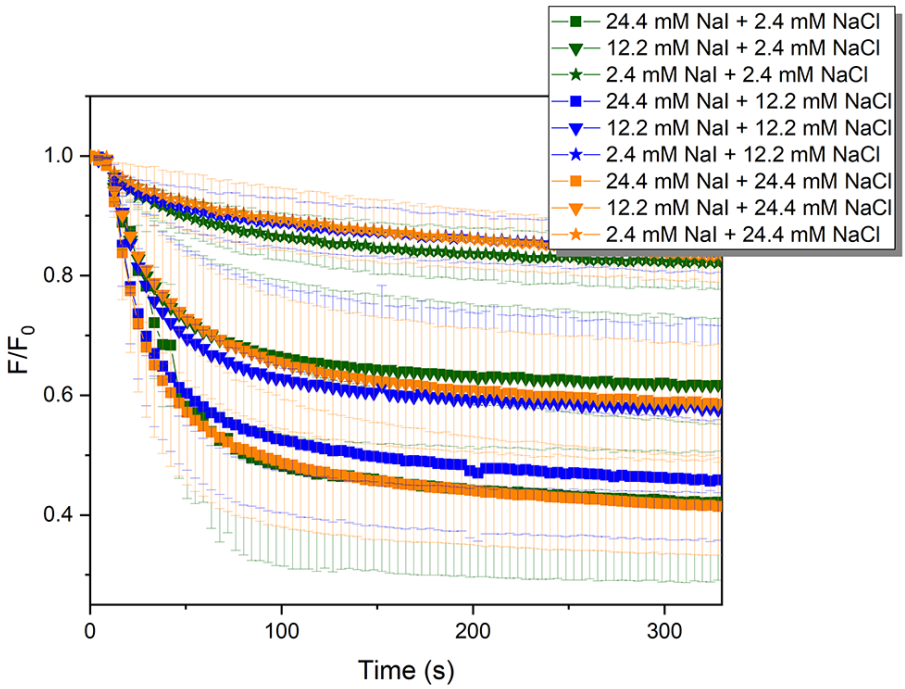

Figure S38. Kinetic anion transport traces of the TLF system based on 7.5 mol% compound **5**. Anion transport involved NaI sample (iodide transport) contaminated with 2.4 mM NaCl (dark green), 12.2 mM NaCl (blue) or 24.4 mM NaCl (orange). Experiments were performed as described in Section S5, and are the average of a minimum of 3 repeats (error bars represent standard deviations).

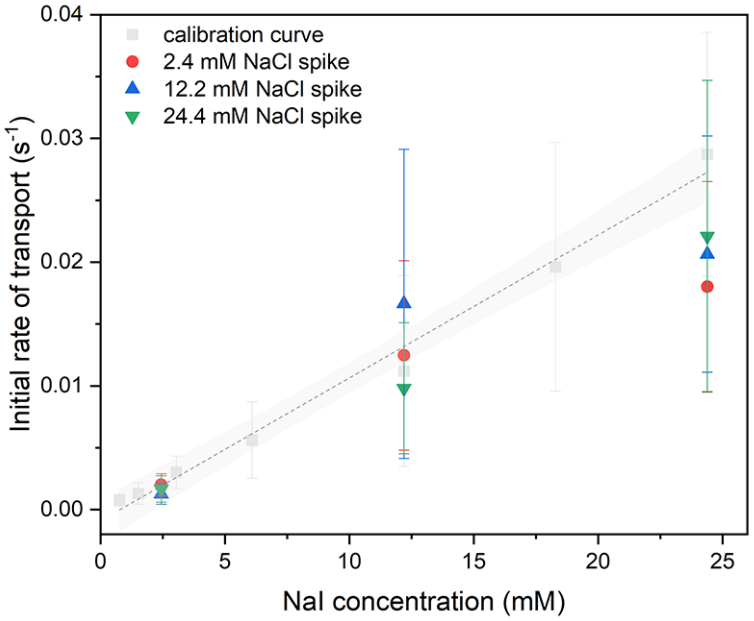

Figure S39. Initial rate of transport obtained from the kinetic anion transport traces shown in Figure S38 overlaid onto the NaI calibration curve for the TLF system based on 7.5 mol% compound **5** (Figure S27). Grey band shows the 95% confidence interval of the calibration curve.

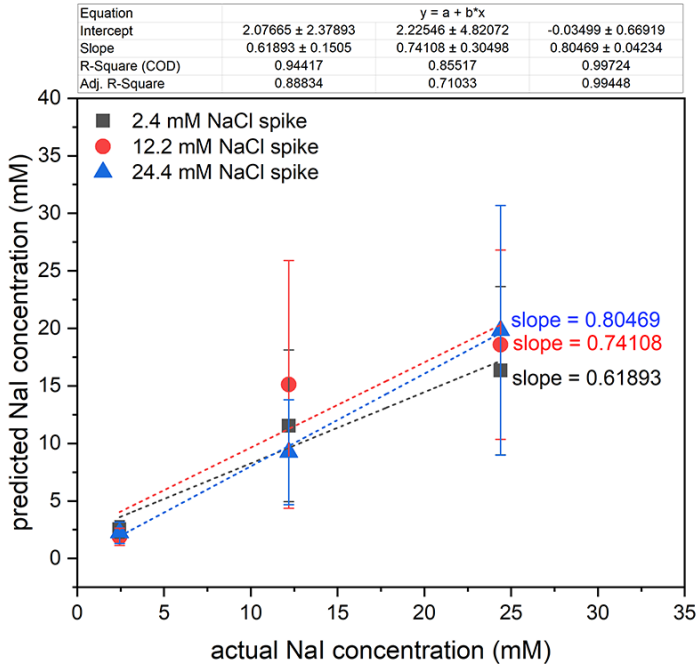

Figure S40. Predicted NaI concentrations (using the calibration curve of Figure 27) versus actual NaI concentration in the NaCl-contaminated samples.

*S8.4. Results for the TLF system based on 5 mol% compound **5***

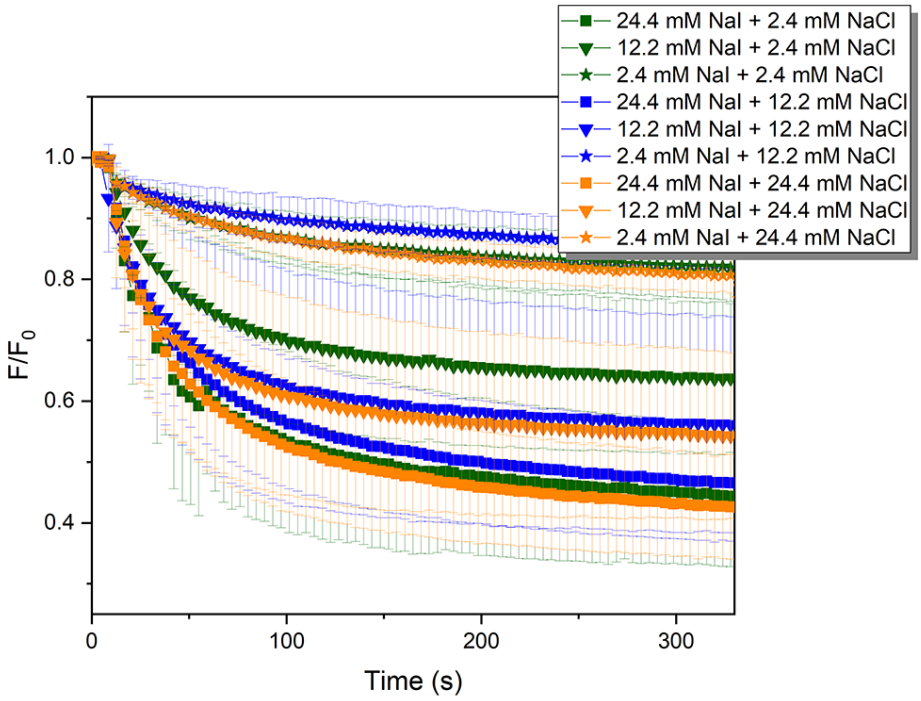

Figure S41. Kinetic anion transport traces of the TLF system based on 5 mol% compound **5**. Anion transport involved NaI sample (iodide transport) contaminated with 2.4 mM NaCl (dark green), 12.2 mM NaCl (blue) or 24.4 mM NaCl (orange). Experiments were performed as described in Section S5, and are the average of a minimum of 3 repeats (error bars represent standard deviations).

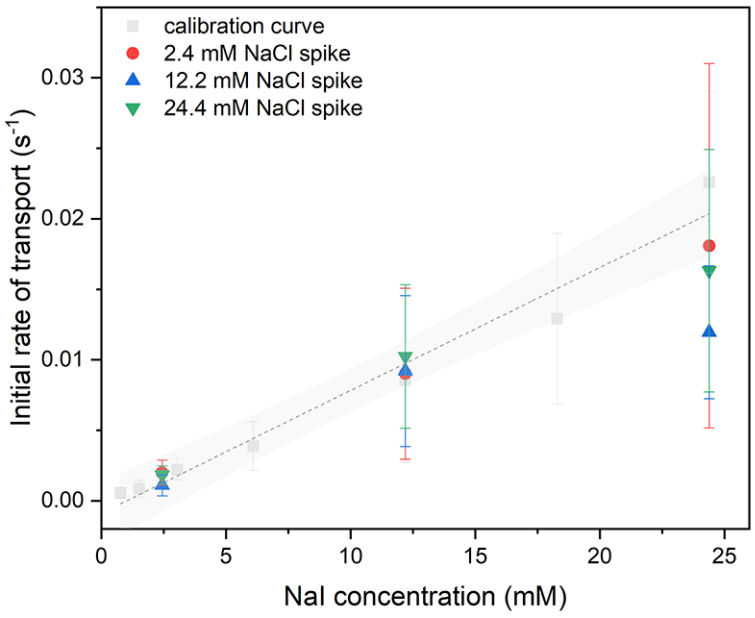

Figure S42. Initial rate of transport obtained from the kinetic anion transport traces shown in Figure S41 overlaid onto the NaI calibration curve for the TLF system based on 5 mol% compound **5** (Figure S28). Grey band shows the 95% confidence interval of the calibration curve.

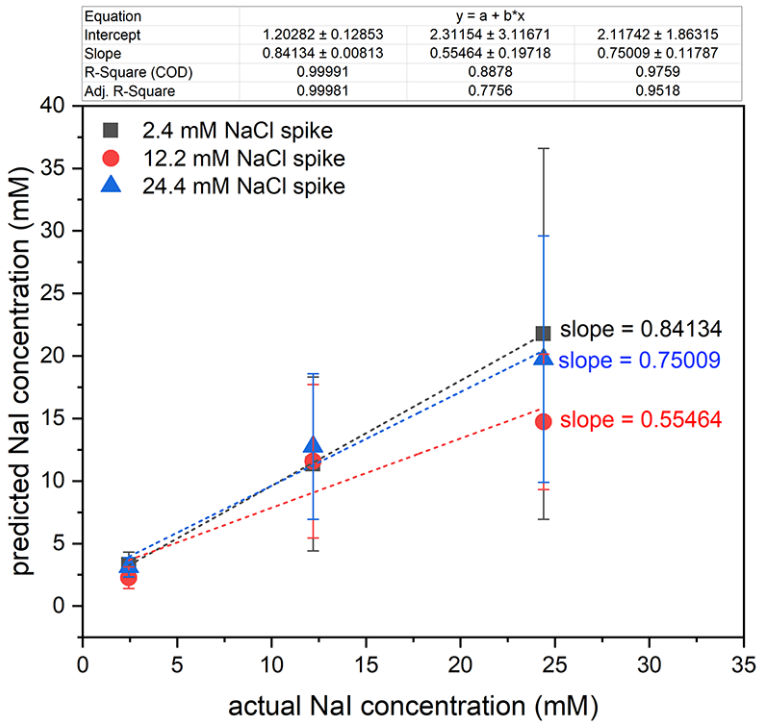

Figure S43. Predicted NaI concentrations (using the calibration curve of Figure S28) versus actual NaI concentration in the NaCl-contaminated samples.

S8.5. Results for the TLF system without transporter (DMF)

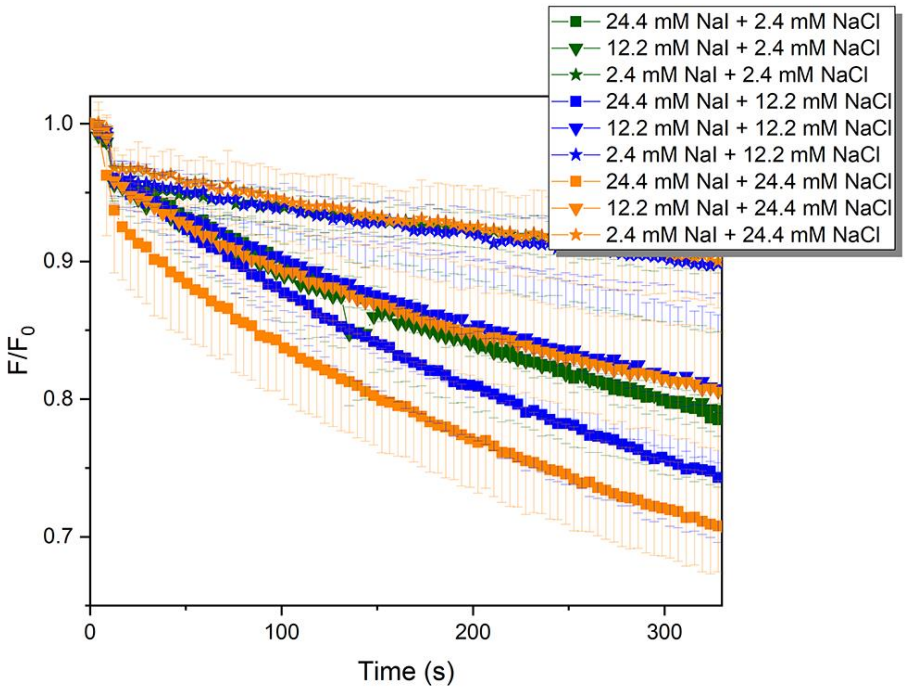

Figure S44. Kinetic anion transport traces of the TLF system without transporter. Anion transport involved NaI sample (iodide transport) contaminated with 2.4 mM NaCl (dark green), 12.2 mM NaCl (blue) or 24.4 mM NaCl (orange). Experiments were performed as described in Section S5, and are the average of a minimum of 3 repeats (error bars represent standard deviations).

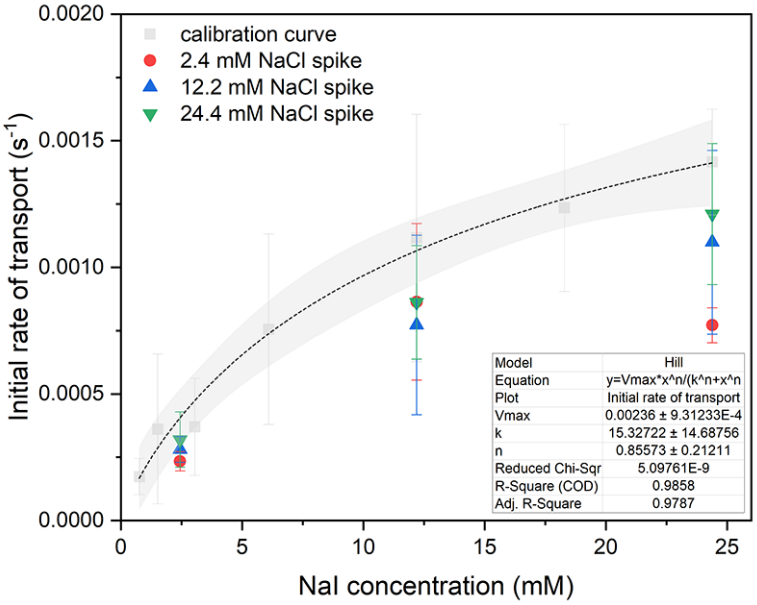

Figure S45. Initial rate of transport obtained from the kinetic anion transport traces shown in Figure S44 overlaid onto the NaI calibration curve for the TLF system without transporter (sigmoidal fit of the range 0 – 25 mM NaI). Grey band shows the 95% confidence interval of the calibration curve.

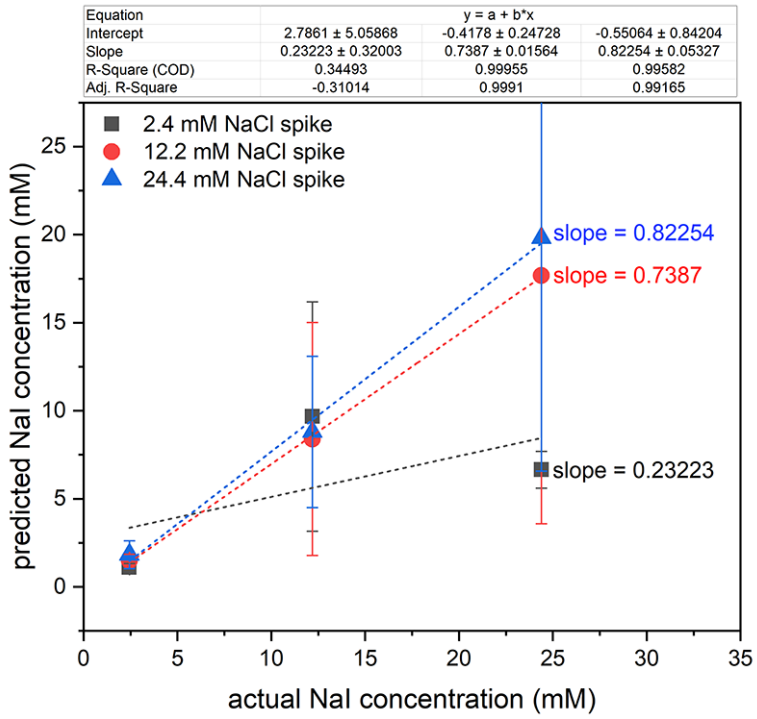

Figure S46. Predicted NaI concentrations (using the sigmoidal fit of the range 0 – 25 mM NaI, Figure S45) versus actual NaI concentration in the NaCl-contaminated samples.

S9. NaI calibration and contaminated samples measured on same liposome batch

The results shown in Sections S7 and S8 (above) gave relatively high error values. This is largely due because they are the result of at least 3 fully independent experiments that were conducted on different batches of liposomes. While this proves the robustness of the approach, for a real-life application it is more accustomed to calibrate the specific batch of liposomes that will be used for the determination of the iodide concentration of an unknown sample. We therefore performed the NaI calibration, and the measurement of NaI samples contaminated with 24.4 mM NaCl on the same day and on the same batch of liposomes. The result for the TLF system based on 4 mol% compound **2** is shown in **Figure S47**, and the result for the TLF system without transporter is shown in **Figure S48**. It is clear that the error is greatly reduced this way and the TLF system based on compound **2** is suitable for the accurate determination of iodide concentrations in complex contaminated samples. For the TLF system without transporter, the values of the NaCl contaminated sample are consistently above the calibration curve, indicating that the small amount of chloride permeability has an effect and that this system cannot be used to accurately determine iodide concentrations. A transporter is thus required in the TLF system to achieve large enough transport rates that can be accurately determined, and to achieve a good dynamic range.

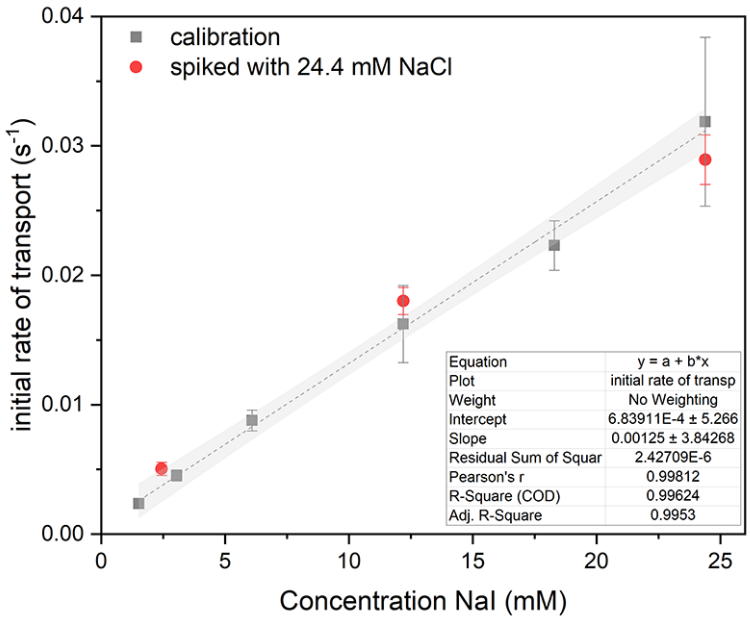

Figure S47. Initial rate of transport obtained for NaI samples contaminated with 24.4 mM NaCl overlaid onto the NaI calibration curve for the TLF system based on 4 mol% compound **2**. Experiments were performed as described in Section S5, and are the average of 3 repeats run on the same day on the same batch of liposomes (error bars represent standard deviations).

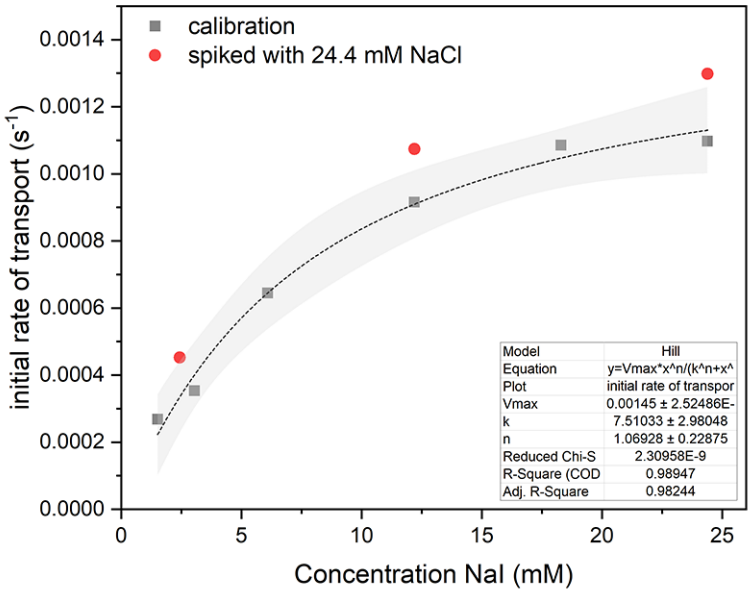

Figure S48. Initial rate of transport obtained for NaI samples contaminated with 24.4 mM NaCl overlaid onto the NaI calibration curve for the TLF system without transporter (neat DMF was added). Experiments were performed as described in Section S5, and are the average of 3 repeats run on the same day on the same batch of liposomes (error bars represent standard deviations).

S10. Determining the final selectivity of the TLF system for iodide detection

So far, the TLF system based on 4 mol% compound **2** was identified as the optimal system, with the best iodide selectivity over other halide anions and the best dynamic range. However, lucigenin is also quenched by some non-halide anions and we therefore wanted to see if this TLF system is selective for iodide over these anions as well. We thus performed the experiment described in Section S5 for the TLF system based on compound **2** with the sodium salts of fluoride, chloride, bromide, iodide, nitrate, sulfate, dihydrogen phosphate, perchlorate, bicarbonate, acetate, gluconate and ascorbate (final concentrations 25 mM). **Figure S49** show the corrected F/F_0 traces obtained for this experiment. All experiments are the average of a minimum of 3 independent repeats (using different batches of liposomes), and error bars indicate standard deviations. The calculated initial rate of transport ($|k_{ini}|$ values) are given in **Table S9**. The bar graph of the initial rate of transport is given in **Figure S50**. The results show that the incorporation of lucigenin into a TLF system based on transporter **2** has increased its selectivity for iodide over other anions.

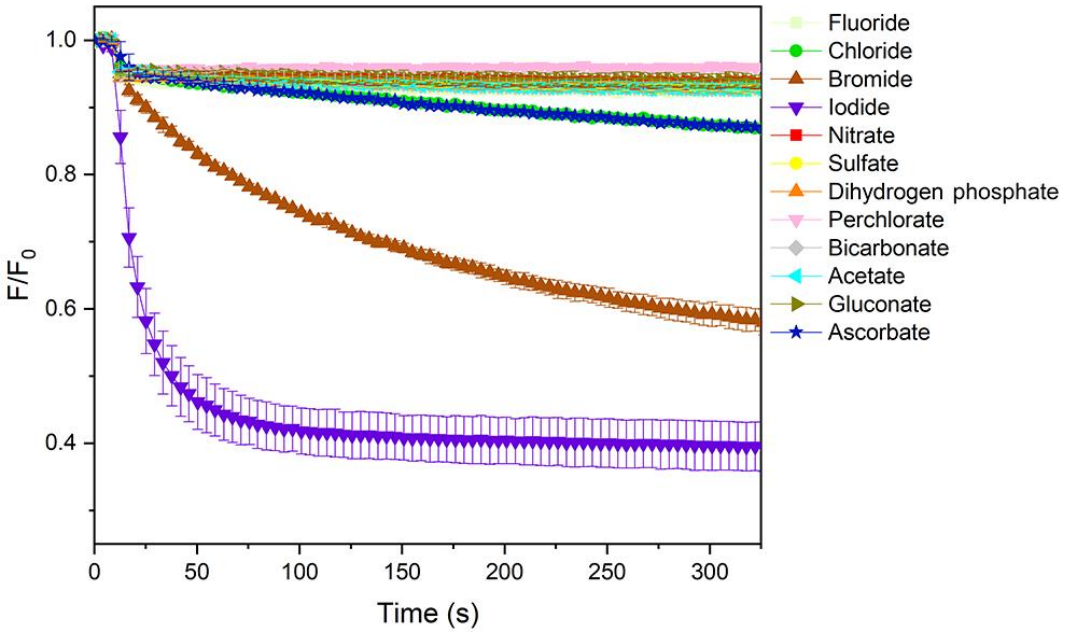

Figure S49. Kinetic anion transport traces of the anion transport mediated by 4 mol% transporter **2** (mol% with respect to lipid). Experiment was performed as described in Section S5, and is the average of a minimum of 3 repeats (error bars represent standard deviations).

Table S9. Absolute initial rate of transport ($|k_{ini}|$) obtained for anion transport mediated by 4 mol% of compound **2** (mol% with respect to lipid). Values are the average of minimum 3 independent repeats. Errors represent standard deviations.

Anion	$\|k_{ini}\|$ in s^{-1}
fluoride	$(1.6 \pm 0.4)\cdot10^{-4}$
chloride	$(3.5 \pm 0.1)\cdot10^{-4}$
bromide	$(2.8 \pm 0.1)\cdot10^{-3}$
iodide	$(3.3 \pm 0.6)\cdot10^{-2}$
nitrate	$(1.5 \pm 0.9)\cdot10^{-4}$
sulfate	$(1.9 \pm 0.2)\cdot10^{-4}$
phosphate	$(1.3 \pm 0.8)\cdot10^{-4}$
perchlorate	$(1.5 \pm 0.1)\cdot10^{-4}$
bicarbonate	$(3.1 \pm 0.3)\cdot10^{-4}$
acetate	$(1.0 \pm 0.5)\cdot10^{-4}$
gluconate	$(1.2 \pm 0.8)\cdot10^{-4}$
ascorbate	$(4.1 \pm 0.9)\cdot10^{-4}$

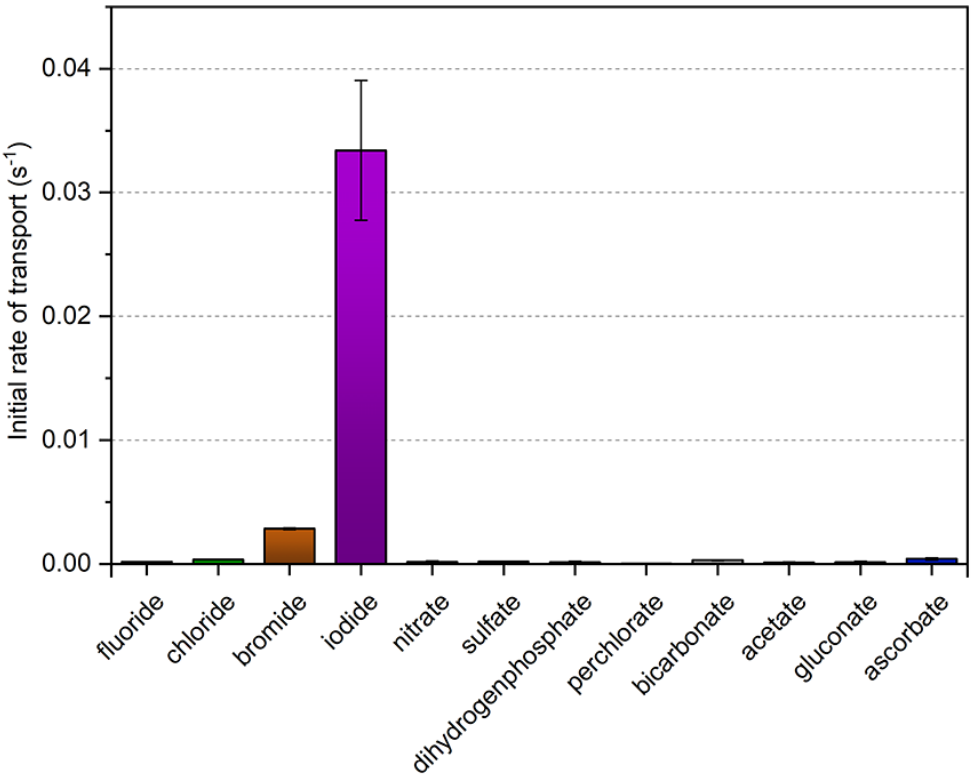

Figure S50. Anion selectivity of the TLF system based on lucigenin, EggPC liposomes and 4 mol% **2** (with respect to EggPC lipid). Experiments and data analysis were performed as described in section S5, using 25 mM as the final concentration of the anions. Results are the average of 3 independent repeats and errors bars represent standard deviations.

S11. References

1. Marcus, Y., *Ions in Solution and their Solvation*. John Wiley & Sons: 2015.
2. Busschaert, N.; Kirby, I. L.; Young, S.; Coles, S. J.; Horton, P. N.; Light, M. E.; Gale, P. A., Squaramides as Potent Transmembrane Anion Transporters. *Angew. Chem. Int. Ed.* **2012,** *51* (18), 4426-4430.
3. Pfeifer, L.; Engle, K. M.; Pidgeon, G. W.; Sparkes, H. A.; Thompson, A. L.; Brown, J. M.; Gouverneur, V., Hydrogen-Bonded Homoleptic Fluoride–Diarylurea Complexes: Structure, Reactivity, and Coordinating Power. *J. Am. Chem. Soc.* **2016,** *138* (40), 13314-13325.
4. Sauer, B.; Skinner-Adams, T. S.; Bouchut, A.; Chua, M. J.; Pierrot, C.; Erdmann, F.; Robaa, D.; Schmidt, M.; Khalife, J.; Andrews, K. T.; Sippl, W., Synthesis, biological characterisation and structure activity relationships of aromatic bisamidines active against Plasmodium falciparum. *Eur. J. Med. Chem.* **2017,** *127*, 22-40.